EurJIC
European Journal of Inorganic Chemistry

Full Paper
doi.org/10.1002/ejic.202000589

Zinc Complexes

Zinc Schiff Base Complexes Derived from 2,2′-Diaminobiphenyls: Solution Behavior and Reactivity towards Nitrogen Bases

Knut Tormodssønn Hylland,*[a] Sigurd Øien-Ødegaard,[a] Richard H. Heyn,[b] and Mats Tilset *[a]

Abstract: Zn complexes of Schiff base ligands derived from 2,2′-diaminobiphenyls and salicylaldehyde derivatives were synthesized and characterized by NMR and single-crystal X-ray diffraction analysis. The detailed NMR studies suggest that the Zn complexes have a complicated behavior in solution, which is strongly dependent on the donating ability of the solvent, the steric properties of the ligand, as well as the concentration of the complex in the solvent. All these factors are decisive for the determination of the coordination number of the complex in solution. Furthermore, pentacoordinated Zn complexes of the aforementioned type, ligated by a series of nitrogen bases, were synthesized. NMR studies of the different complexes at different concentrations and temperatures, revealed information about their conformational stability. The differences were further examined by single-crystal X-ray diffraction analysis. In addition to the studies conducted on Zn complexes, comparative studies were conducted on a series of Cd complexes.

Introduction

Schiff base complexes of Zn find application within catalysis,[1] supramolecular chemistry,[2] chemical sensing and recognition.[3] These applications take advantage of the Lewis acidic character of Zn.[4] Especially salen and salphen complexes of Zn (**I**, **II** and **III**, Figure 1) have been well-studied.[5] 2,2′-diaminobiphenyls represent an interesting class of precursors for Schiff base complexes, e.g. of Zn (**IV**, Figure 1). In addition to having the amino groups positioned in such a manner that a salen-like chelate can be constructed, they have inherent chirality that can be exploited for the synthesis of enantiopure ligands and metal complexes.[6] Furthermore, the linear nature of the biphenyl backbone may facilitate incorporation in metal organic frameworks[7] and other materials, if additional functionality that allows for heterogenization is present in the diamine (e.g. carboxylic acids). Finally, and maybe of highest practical importance, the biphenyl backbone is readily functionalized, and many derivatives are accessible by standard methods in organic chemistry.[8]

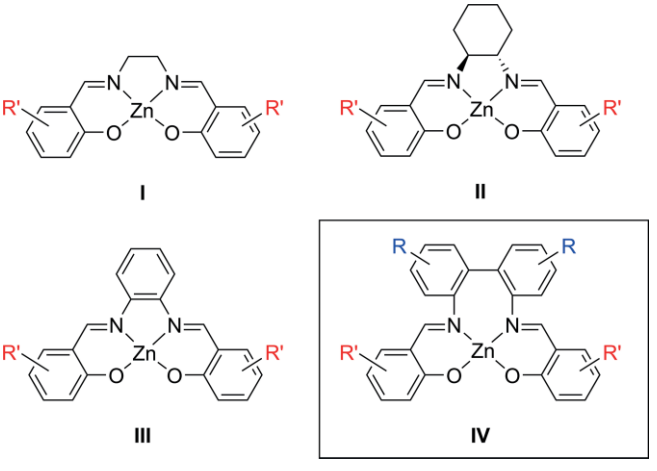

Figure 1. General structure of Zn salen (**I** and **II**) and Zn salphen complexes (**III**), and Zn Schiff base complexes presented herein (**IV**).

As a consequence of their Lewis acidity, Zn salen and salphen complexes exhibit an often complicated behavior in solution, largely influenced by the donating ability of the solvent.[9] Di Bella and co-workers did extensive studies, both experimentally[4d,10] and computationally,[4a] on Zn salen and salphen complexes. They found that these complexes have a strong tendency to form dimers, oligomers or higher aggregates in the absence of a donating solvent. Interestingly, the tendency to form aggregates was found to be strongly influenced by the nature of the bridging amine in the ligand backbone.[4d,5b] It was also shown that the aggregation was reversible, and that

[a] K. T. Hylland, Dr. S. Øien-Ødegaard, Prof. M. Tilset
Department of Chemistry, University of Oslo,
P. O. Box 1033 Blindern, 0315 Oslo, Norway
E-mail: k.t.hylland@smn.uio.no
mats.tilset@kjemi.uio.no
http://www.mn.uio.no/kjemi/personer/vit/matst/index.html
[b] Dr. R. H. Heyn
SINTEF Industry,
P.O. Box 124 Blindern, 0314 Oslo, Norway
Supporting information and ORCID(s) from the author(s) for this article are available on the WWW under https://doi.org/10.1002/ejic.202000589.
© 2020 The Authors published by Wiley-VCH GmbH • This is an open access article under the terms of the Creative Commons Attribution License, which permits use, distribution and reproduction in any medium, provided the original work is properly cited.

© 2020 The Authors published by Wiley-VCH GmbH

Full Paper
doi.org/10.1002/ejic.202000589

monomeric pentacoordinated complexes would form on addition of a suitable ligand, e.g. DMSO or pyridine.[4a,4d]

The coordination chemistry of salen-type Zn complexes towards different nitrogen bases have been studied extensively. Kleij and co-workers reported the adsorption of nicotine and related alkaloids by Zn salphen complexes.[3a] The same group has also studied the interaction between Zn salphen complexes and biologically relevant heterocycles,[11] as well as the construction of supramolecular assemblies based on the interaction between Zn complexes and heterocycles.[2e] In addition, Schiff base complexes of Zn find application as catalysts for different reactions between CO_2 and epoxides.[12] For these reactions (copolymerization and cycloaddition), nitrogen-containing bases are occasionally used as co-catalysts,[1f,12a,13] thus studies of the interaction between Zn complexes and nitrogen bases are of relevance for this field as well.

Herein, in-depth studies of Zn complexes of Schiff bases of 2,2′-diaminobiphenyl derivatives will be presented. The emphasis will be on NMR studies of their behavior in solution, their reactivity towards different nitrogen-containing bases, and the crystallographic structure determination of the obtained complexes. In addition, a preliminary study of the corresponding Cd complexes will be presented and comparisons with the Zn complexes will be made.

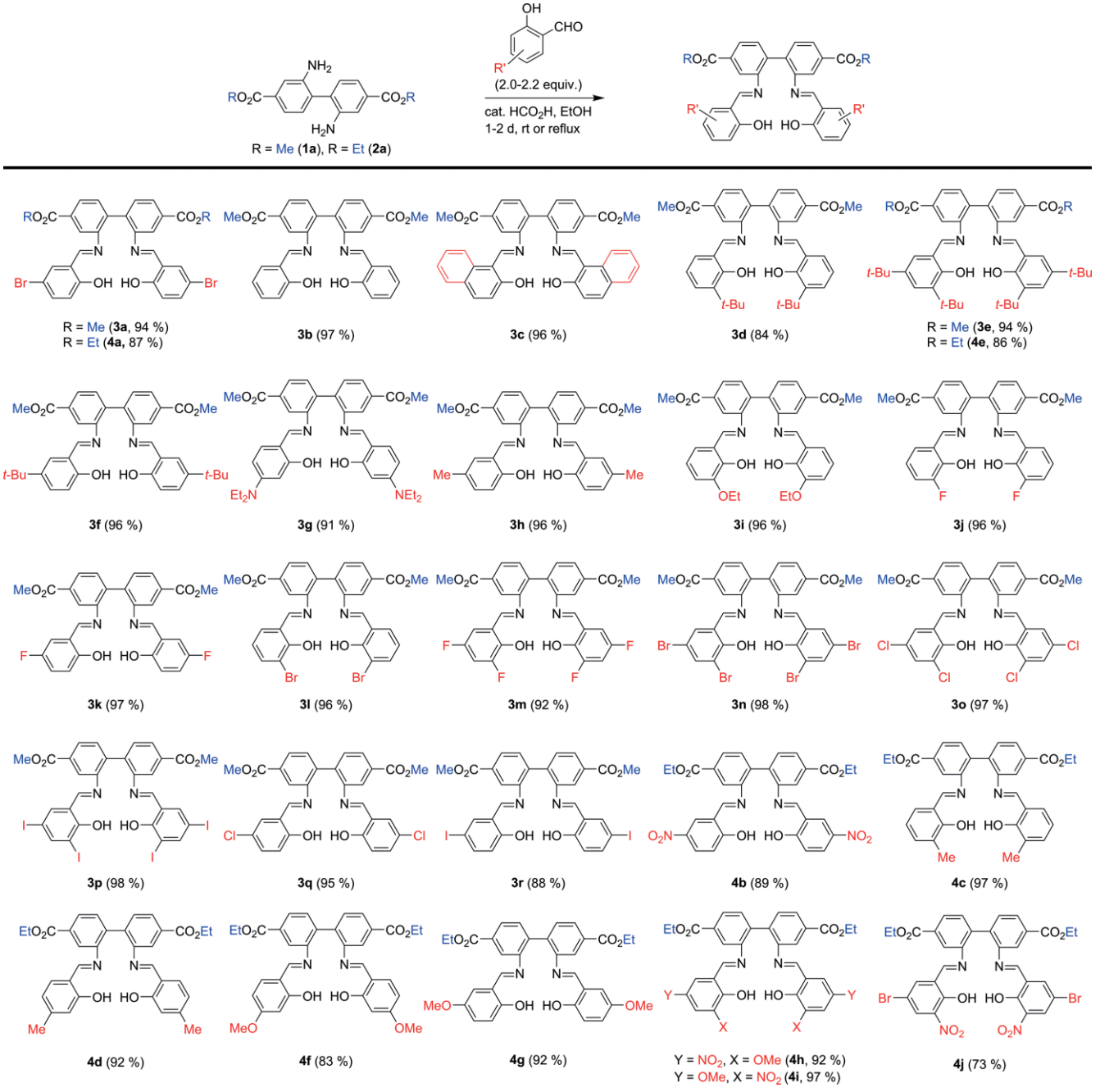

Scheme 1. Synthesis of Schiff base ligands **3a**–**3r** and **4a**–**4j** from 2,2′-diaminobiphenyls **1a** and **2b**.

© 2020 The Authors published by Wiley-VCH GmbH

Full Paper
doi.org/10.1002/ejic.202000589

Results and Discussion

Synthesis of Zn Complexes of Tetradentate Schiff Base Ligands

Two 2,2′-diaminobiphenyls were chosen as suitable amine precursors for the synthesis of Schiff base complexes of Zn; dimethyl 2,2′-diaminobiphenyl-4,4′-dicarboxylate (**1a**) and diethyl 2,2′-diaminobiphenyl-4,4′-dicarboxylate (**2a**) (see SI for details). In addition to having the required amino substituents, they also carry functionality that may permit the heterogenization of the complexes (although not accounted for in this article). The two diamines **1a** and **2a** were conveniently synthesized in two- and three-step procedures from commercially available starting materials, using modified literature procedures.[8h,14] All reactions could be performed on a large scale (yielding 15–20 gram of final products **1a** and **2a**), and all compounds could be recrystallized to yield pure products. The diamines **1a** and **2a** were subjected to reactions with different

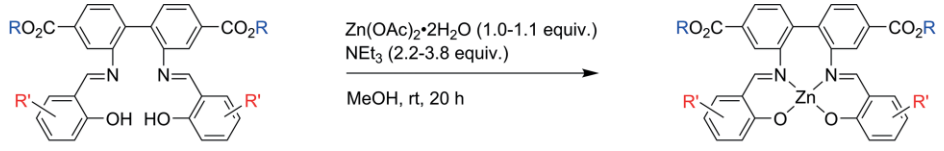

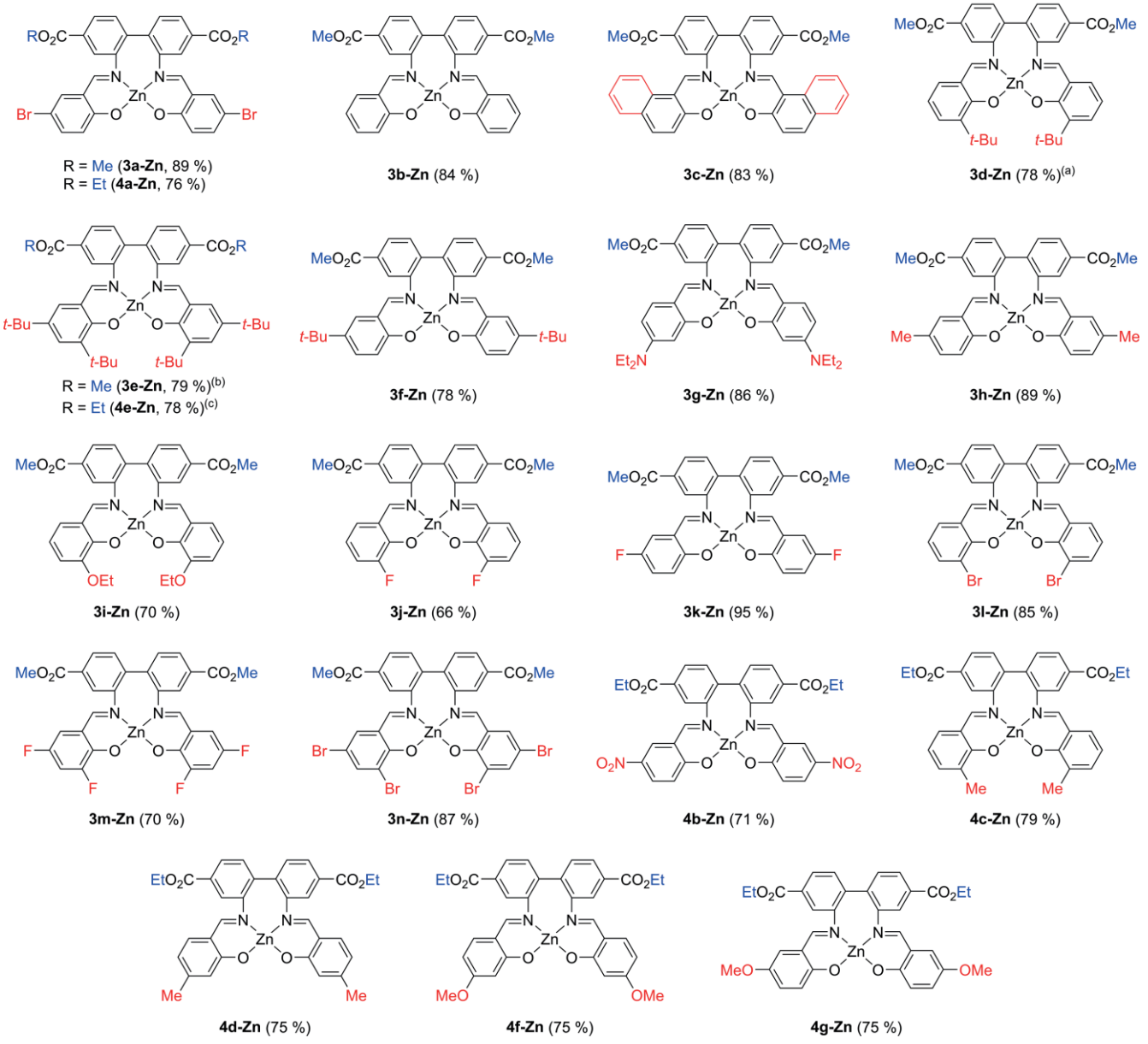

Scheme 2. Synthesis of Zn complexes **3a-Zn**–**3m-Zn** and **4a-Zn**–**4g-Zn**. [a] CH_2Cl_2 was used as co-solvent. [b] *tert*-Butyl-1,1,3,3-tetramethylguanidine was used as base instead of NEt_3. [c] iPr_2NEt was used as base instead of NEt_3.

© 2020 The Authors published by Wiley-VCH GmbH

Full Paper
doi.org/10.1002/ejic.202000589

salicylaldehydes according to standard literature procedures,[15] furnishing the corresponding Schiff base ligands **3a**–**r** and **4a**–**j** (Scheme 1).

Two of the ligands, **3b** and **3e**, were structurally characterized (see SI). As many salicylaldehyde derivatives are commercially available, a variety of ligands with different electronic and steric properties could be synthesized in a relatively straightforward manner, which avoids time-consuming work-up and purification protocols. Zn complexes of these Schiff base ligands were synthesized by reacting the appropriate ligand with one equivalent of $Zn(OAc)_2{\cdot}2H_2O$ in methanol, in the presence of an excess of NEt_3 (Scheme 2).

These reaction conditions are fairly general for the synthesis of Zn complexes of related Schiff bases.[1b,3c,16] The protocol avoids the use of air sensitive starting materials (diethyl- or dimethylzinc) and dry solvents, which occasionally are reported in the literature for the synthesis of similar complexes,[1f,17] making it a convenient method which could be performed on both smaller (0.5 mmol) and larger (10 mmol) scale. The complexes were characterized by NMR spectroscopy (vide infra) and MS, as well as IR, elemental analysis and single-crystal X-ray diffraction analysis for selected complexes.

Single-Crystal X-ray Diffraction Analysis of Complex 4a-Zn

One of the complexes in Scheme 2, **4a-Zn,** was studied by single-crystal X-ray diffraction analysis. The complex crystallized as a monomer with distorted tetrahedral geometry around Zn (Figure 2) and its asymmetric unit consisted of two molecules. The Zn–N and Zn–O bond lengths are similar to what has been reported previously by Constable and co-workers for a related tetrahedral Zn complex of a Schiff base derived from 2,2′-diamino-1,1′-binaphthyl,[18] although the bond angles are somewhat deviating. This could probably be attributed to differences between the biphenyl and the binaphthyl backbone. Although the geometry of **4a-Zn** can be described as tetrahedral, it is severely distorted as reflected by its τ_4' values,[19] which was found to be 0.56 and 0.61 for each of the two complexes in the asymmetric unit.

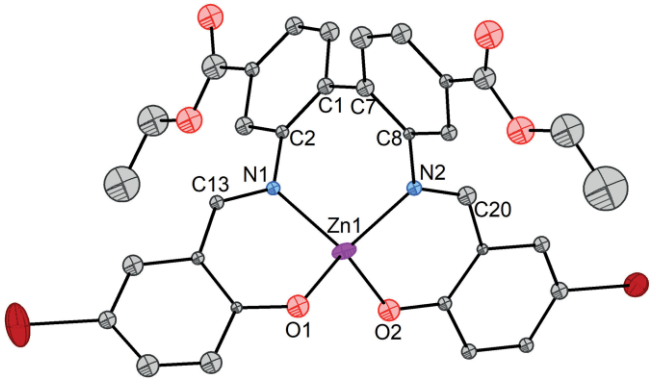

Figure 2. ORTEP plot of **4a-Zn**. Because of disorder limiting the high-resolution diffraction in the measured crystal, only Zn and Br are refined as thermal ellipsoids (set at 50 % probability). Only one of the two molecules of the asymmetric unit is displayed, but metric data for both are given below. Hydrogen atoms have been omitted for clarity. $\tau_4' = 0.56, 0.61$. Selected bond lengths [Å] and angles [°]: Zn1–N1, 2.0217(4); Zn1–N2, 2.0046(4); Zn1–O1, 1.9334(3); Zn1–O2, 1.8789(3); N1–C13, 1.2851(3); N2–C20, 1.2939(2); Zn2–N3, 2.0111(4); Zn2–N4, 2.0271(3); Zn2–O3, 1.9021(4); Zn2–O4, 1.9015(3); N1–Zn1–N2, 96.373(13); N1–Zn1–O1, 94.137(13); N1–Zn1–O2, 140.589(16); N2–Zn1–O1, 140.296(15); N2–Zn1–O2, 94.620(14); O1–Zn1–O2, 101.090(14); C2–C1–C7–C8, 62.722(33); N3–Zn2–N4, 94.647(13); N3–Zn2–O3, 94.996(14); N3–Zn2–O4, 141.412(16); N4–Zn2–O3, 133.220(15); N4–Zn2–O3, 95.295(13); O3–Zn2–O4, 104.776(14).

The distorted tetrahedral geometry around Zn found in the structure of **4a-Zn**, together with the findings of Constable and co-workers,[18] is interesting as it suggests that the Zn Schiff base complexes discussed herein are much more prone to exist as monomeric tetracoordinated species than e.g. Zn salphen complexes. Crystal structures of tetracoordinated Zn in salphen and salen complexes are rare, and only few examples are known.[3e,4e] However, in the literature it was found that Zn is tetracoordinated in Schiff base complexes derived from chiral diamino backbones, e.g. *trans*-1,2-diaminocyclohexane, forming double-helicate dimeric Zn_2L_2 structures.[5b,20]

NMR Studies of 4a-Zn and Other Zn Complexes

Knowledge of the behavior of a metal complex in solution is valuable for many applications, e.g. catalysis. Hence, complex **4a-Zn** was subjected to detailed NMR studies. Large differences in the ^{1}H NMR resonances of the complex were observed going from weakly donating solvents ($CDCl_3$) to strongly donating solvents ([D_6]DMSO). In $CDCl_3$, a strong concentration dependency was found for the appearance of the ^{1}H NMR resonances of **4a-Zn**. At low concentrations of the complex, the resonances were relatively sharp, and with similar chemical shifts as those observed for ligand **4a**. On increasing the concentration however, all the resonances became broadened. In addition, some of the resonances were moved to lower ppm values (Figure 3). Similar observations were made in C_6D_6 and [D_6]acetone (Figure S183 and Figure S184, SI).

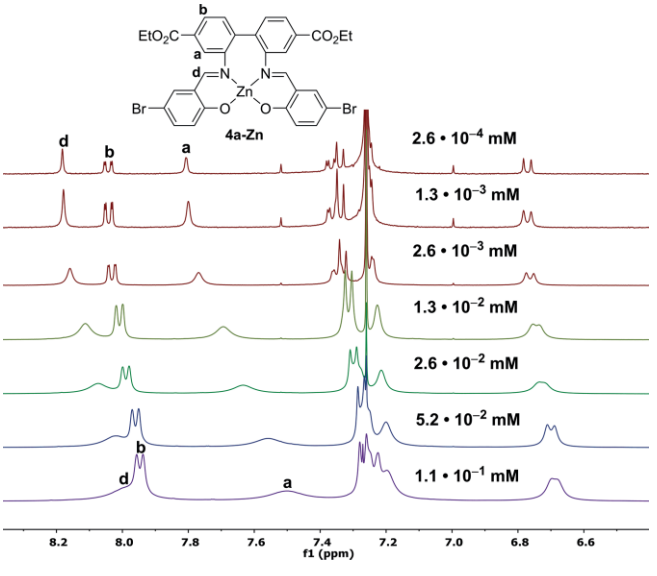

Figure 3. Stacked ^{1}H NMR (400 MHz, $CDCl_3$) spectra of **4a-Zn** at different concentrations. Only the aromatic region is shown.

© 2020 The Authors published by Wiley-VCH GmbH

Full Paper
doi.org/10.1002/ejic.202000589

The increased shielding of the ^{1}H NMR resonances on increasing the concentration of **4a-Zn** was especially evident for the protons in close proximity to Zn (H^a and H^d, see Figure 3). Upon increasing the concentration, the chemical shift for H^a changes from 7.81 ppm to 7.50 ppm, which is significant for a *non*-interchangeable proton.[21] In [D_6]DMSO on the other hand, the ^{1}H NMR resonances of **4a-Zn** were sharp and well-defined at all concentrations studied (see Figure S169, SI). The observed differences in the two solvents could be explained by that DMSO is a strongly donating ligand, and when dissolved in [D_6]DMSO, **4a-Zn** would exist solely as the pentacoordinated monomeric complex **4a-Zn-[D_6]DMSO**. $CDCl_3$ however is a significantly less donating solvent, and other processes would hence dominate. NMR studies of related Zn salen and salphen complexes in the literature suggest that these are prone to form dimers, oligomers or higher aggregates in poorly donating solvents.[2c,4a,4d,17] Due to the structural similarities between Zn salen and salphen complexes, and the complexes studied herein, these processes may also be relevant for **4a-Zn**. The ^{1}H NMR spectra presented in Figure 3 may indicate that different species are present in $CDCl_3$ at different concentrations of **4a-Zn**. At moderate to high concentrations, dimers or higher oligomers of **4a-Zn** may be present, whereas under dilute conditions, a monomeric species may exist. The reversibility of these processes for related Zn salen and Zn salphen complexes have been reported,[2c,10,22] and a model of the process is outlined in Scheme 3.

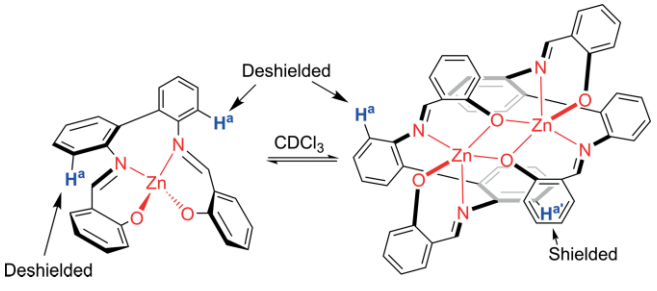

Scheme 3. Model showing the reversible dimerization of **4a-Zn**. The concentration of the complex in $CDCl_3$ is crucial for which species are favored. Bromine atoms and ethoxycarbonyl substituents have been omitted for clarity.

In the tetracoordinated monomer depicted to the left in Scheme 3, the two equivalent protons H^a would be expected to appear at similar chemical shifts in ^{1}H NMR as the corresponding protons in the free ligand **4a**. In the pentacoordinated dimer to the right in Scheme 3, the salicylaldiminato half-units of **4a-Zn** would no longer be equivalent, and the protons H^a would appear as the pair H^a/$H^{a'}$, where one of the protons would be more shielded than the other. The broadened ^{1}H NMR resonances observed at higher concentration of **4a-Zn** may be caused by either an interconversion between the monomer and the dimer, or an interconversion between different dimers or oligomers (vide infra). At low concentrations of **4a-Zn**, the chemical shift corresponding to H^a appears at 7.81 ppm, which indicates negligible shielding (Scheme 3), and it is comparable to what is observed for ligand **4a** in $CDCl_3$ (7.89 ppm). On the other hand, the chemical shift at moderate to high concentration of **4a-Zn** in $CDCl_3$ is comparable with what is observed for H^a in the presumably pentacoordinated **4a-Zn-[D_6]DMSO** in [D_6]DMSO (7.61 ppm, see Experimental Section) as well as for the same proton of pentacoordinated complexes of **3d-Zn**, **3e-Zn** and **4e-Zn** (vide infra). From this, it is most likely that tetracoordination is found for **4a-Zn** at low concentrations of the complex in $CDCl_3$, and that pentacoordination is dominant at higher concentrations. As **4a-Zn** was found to exhibit dynamic behavior throughout the whole range of concentrations that was studied, it is reasonable to assume that a dimeric state is only intermediate, and that an oligomer or a mixture of oligomers are present under the most concentrated conditions (which is in agreement with the extensive broadening observed). From MS, *m/z* values corresponding to dimeric species could be observed for some of the Zn complexes studied herein (see SI), but no higher oligomers could be detected by this method.

The resonances of each of the salicylaldiminato half-units in **4a-Zn** appeared as equivalent in the ^{1}H NMR spectrum of the Zn complex in [D_6]DMSO. Whereas a tetracoordinated compound may be present at very low concentrations of **4a-Zn** in $CDCl_3$, the above assumption about the coordination of a solvent molecule to **4a-Zn** in [D_6]DMSO, would necessarily result in a pentacoordinated geometry around Zn. For pentacoordinated Schiff base complexes of Zn, both square pyramidal[2a] and trigonal bipyramidal[3c] geometries are common. Pentacoordinated metal complexes are known to be stereochemically non-rigid species,[23] and molecules with trigonal bipyramidal geometry are known to isomerize by the Berry pseudorotation mechanism.[24] Judging from the ^{1}H NMR spectrum of **4a-Zn** in [D_6]DMSO, this process may occur very rapidly at ambient temperature, leading to a sharp set of time-averaged resonances in the ^{1}H NMR spectrum. At the concentrations of **4a-Zn** in $CDCl_3$ where the complex seemed highly susceptible to undergo dimerization/oligomerization (Figure 3, 2.6×10^{-3} mM to 1.1×10^{-1} mM), the ^{1}H NMR spectra of **4a-Zn** showed broadened to very broadened resonances. Applying the pseudorotation mechanism on such a dimeric species might account for the broadened signals observed in ^{1}H NMR, indicating that the size and the properties of the fifth ligand at Zn is of crucial importance to how fast this isomerization takes place (Scheme 4).

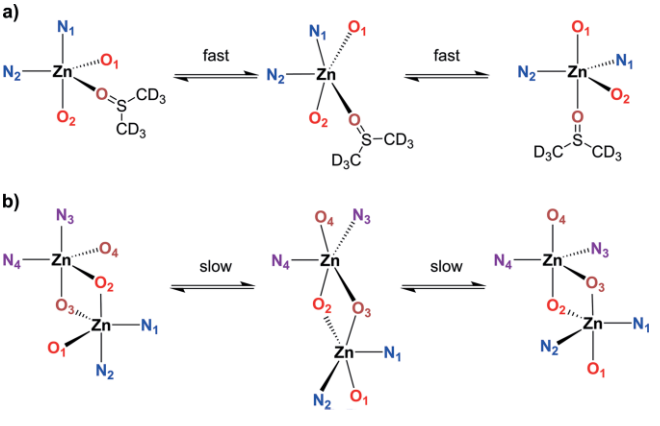

Scheme 4. Proposed pseudorotation of (a) **4a-Zn-[D_6]DMSO** and (b) dimeric **4a-Zn**.

© 2020 The Authors published by Wiley-VCH GmbH

Full Paper
doi.org/10.1002/ejic.202000589

Observations from variable temperature ^{1}H NMR studies of **4a-Zn** in $CDCl_3$ at three different concentrations (2.6×10^{-4} mM, 1.3×10^{-2} mM and 1.1×10^{-1} mM) were in favor of the above assumptions. At the lowest concentration of **4a-Zn** studied, the ^{1}H NMR resonances of the complex underwent minimal changes, and no decoalescence of any resonances could be observed at –56 °C (Figure S173, SI). This supports the assignment of tetracoordination around Zn,[25] and the preservation of the pseudo-C_2 symmetry of the complex observed from the structural characterization. At higher concentrations of **4a-Zn**, broadened resonances were observed at ambient temperature, and decoalescence of the resonances was observed on decreasing the temperature (< –8 °C), indicating that the process outlined in Scheme 4b may be operating.[24c] The complexity of the obtained spectra also suggest that there are several equilibrating complexes present, although it was not possible to unambiguously identify the different species. For more information about the variable temperature NMR studies of **4a-Zn**, see Figure S174 and Figure S175, SI.

In order to gain more insight into which factors that are of importance for dimer formation, a series of Zn complexes with different substituents on the phenolic rings were subjected to NMR studies (Figure 4).

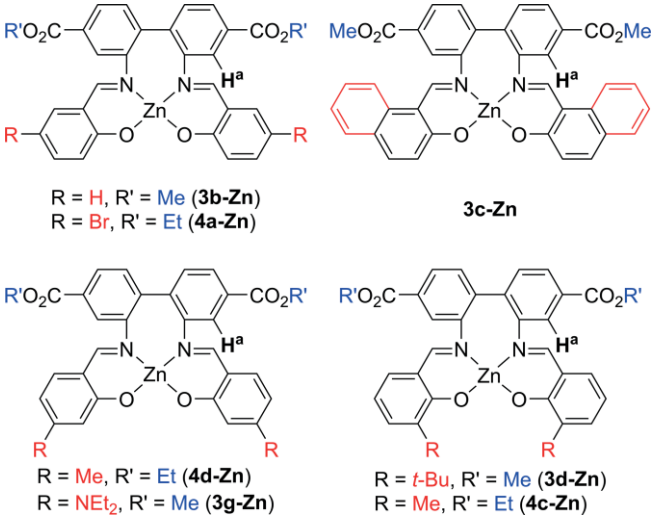

Figure 4. A selection of the different Zn complexes studied herein. The proton H^a of the biphenyl backbone is marked as it is of importance for the discussion (see text).

For complexes carrying substituents *para* to the phenoxides (as well as no substituents; complex **3b-Zn**), similar behavior as was found for **4a-Zn** in $CDCl_3$ was observed. The ^{1}H NMR resonances of the Zn complexes with *ortho* substituents were found to be essentially concentration independent in $CDCl_3$, indicating static behavior under these experimental conditions (see Figure S129 and Figure S194, SI, for concentration studies of **3d-Zn** and **4c-Zn**). In addition, no significant temperature dependency was found for the ^{1}H NMR resonances of **3d-Zn**, when the complex was studied at low temperatures (–44 °C), similar to what was observed for **4a-Zn** at low concentrations in $CDCl_3$ (Figure S130, SI). For complexes carrying substituents *meta* to the phenoxides, no clear trend was observed, and the size of the substituents were found to be of crucial importance for the ^{1}H NMR spectra of the complexes in $CDCl_3$. For complex **4d-Zn** with small methyl substituents, the behavior in $CDCl_3$ was similar to that of **4a-Zn** and **3b-Zn**, whereas naphthalene-substituted complex **3c-Zn** and diethylamino-substituted complex **3g-Zn** behaved similar to complexes with *ortho* substituents, **3d-Zn** and **4c-Zn**. Especially relevant for these studies was the chemical shift values of proton H^a (see Figure 4). The chemical shift was observed at relatively high ppm values for complexes **3c-Zn**, **3d-Zn**, **4c-Zn** and **3g-Zn** independent of concentrations (7.94 ppm, 7.83 ppm, 7.84 ppm and 7.80 ppm respectively). From the dimerization model depicted in Scheme 3, this proton would be anticipated to be strongest influenced by dimerization, and would have been expected to appear at a lower ppm value in a dimer. Indeed, at high concentrations of **4a-Zn** and **4d-Zn**, the resonances corresponding to H^a were found at 7.49 ppm and 7.52 ppm respectively, whereas at very low concentrations, the resonances were found at 7.81 ppm and 7.82 ppm, similarly to what was observed for **3d-Zn**, **4c-Zn** and **3g-Zn** at any concentrations. In summary, these observations suggest that the existence of monomeric tetracoordinated Zn complexes in $CDCl_3$ is very sensitive to the substitution pattern near Zn. In [D_6]DMSO, the ^{1}H NMR spectra of all complexes were similar, and for the 21 different Zn complexes depicted in Scheme 2, the chemical shift range of H^a was only 7.55–7.68 ppm, seemingly being dictated by the electronic properties of the different substituents of each complex.

Coordination of *N*-Ligands to Zn Complexes

To gain deeper knowledge of the coordination of additional ligands to the Zn complexes discussed so far, a series of pentacoordinated complexes were synthesized and studied by NMR and single-crystal X-ray diffraction analysis. Various complexes were studied (see Scheme S6, SI), but the findings will mainly be discussed for complex **3d-Zn** (Figure 4) and the related complexes **3e-Zn** and **4e-Zn** (Scheme 2), and their reactions towards some of the nitrogen-containing bases depicted in Figure 5.

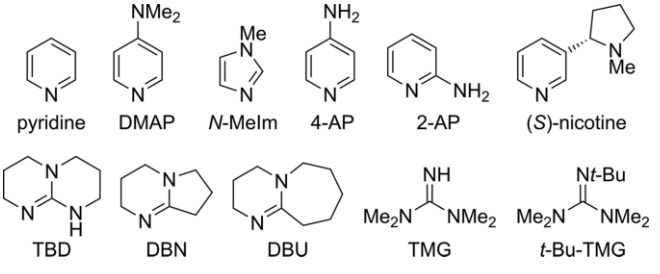

Figure 5. Nitrogen-containing ligands studied in this work.

The bases depicted in Figure 5 all contain a sp^2-hybridized nitrogen atom. Such bases have been reported to coordinate to Zn in related salen and salphen complexes, and several of these Zn complexes have been structurally characterized.[2c,3a,5,11] In addition, there is large diversity in basicity and steric properties for such ligands; from weakly basic pyridine with low steric bulk, to the larger and more basic bicyclic ami-

© 2020 The Authors published by Wiley-VCH GmbH

Full Paper
doi.org/10.1002/ejic.202000589

dines and guanidines 1,5-diazabicyclo[4.3.0]non-5-ene (DBN), 1,8-diazabicyclo[5.4.0]undec-7-ene (DBU) and 1,5,7-Triazabicyclo[4.4.0]dec-5-ene (TBD).[26] *N*-ligated complexes of **3d-Zn** could be synthesized by two methods. For DBU, DBN and TBD, the corresponding complexes **3d-Zn-DBU**, **3d-Zn-DBN** and **3d-Zn-TBD** could be obtained directly from ligand **3d**, by reaction with $Zn(OAc)_2{\bullet}2H_2O$ in the presence of an excess of the given base (Scheme 5a). The similar synthesis of DBU-ligated Zn-phthalocyanine complexes has been reported earlier by Mele and co-workers.[27] Pentacoordinated complexes of **3d-Zn** could also be obtained by recrystallization of the complex in MeCN in the presence of an excess of base (Scheme 5b). Kleij and co-workers used a similar approach for the synthesis of base-ligated Zn salphen complexes.[11]

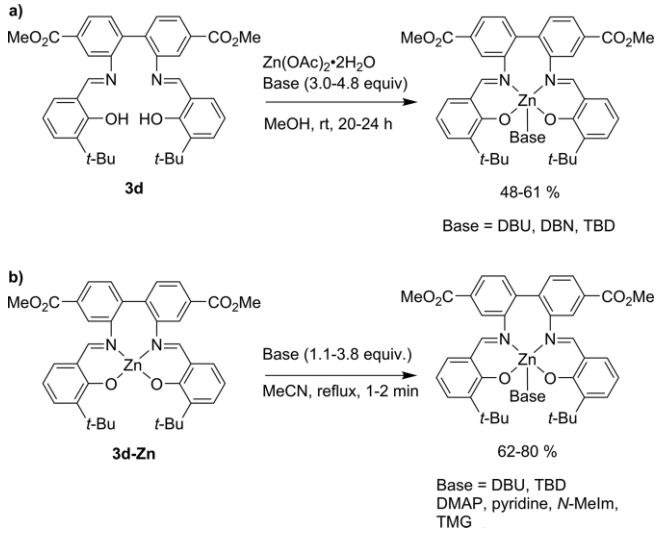

Scheme 5. Synthesis of various base-ligated complexes of **3d-Zn**.

The method depicted in Scheme 5b was suitable for ligation of pyridine, 4-(dimethylamino)pyridine (DMAP), *N*-methylimidazole (*N*-MeIm) and 1,1,3,3-tetramethylguanidine (TMG) to **3d-Zn**, giving access to the complexes **3d-Zn-pyridine**, **3d-Zn-DMAP**, **3d-Zn-*N*-MeIm** and **3d-Zn-TMG**, respectively. The two complexes **3d-Zn-DBU** and **3d-Zn-TBD** could also be obtained by this method. The complexes were characterized by NMR spectroscopy and MS, as well as elemental analysis and single-crystal X-ray diffraction analysis for selected complexes. The interaction between (*S*)-nicotine and **4e-Zn** was studied exclusively by ^{1}H NMR, this was also done for 4-aminopyridine (4-AP) and 2-aminopyridine (2-AP) (see SI). In addition, from ^{1}H NMR studies of the electron poor complex **4b-Zn** in the presence of NEt_3, there were indications of formation of an Zn-NEt_3 adduct (Figure S354, SI). For less electron poor complexes (**3d-Zn** and **4d-Zn**), there were no indications of adduct formation with NEt_3 (Figure S132 and Figure S199, SI). The inability to isolate any Zn complexes ligated by NEt_3 is in agreement with the low affinity of tertiary acyclic amines for Zn in salen and salphen complexes, as reported in the literature,[1e,3d,4e] although Kleij and co-workers were able to structurally characterize an NBu_3-ligated Zn salphen complex.[28] The very sterically hindered base *t*Bu-TMG failed to give any detectable pentacoordinated adducts on reaction with various Zn complexes, but was found to be a useful strong base for the synthesis of complex **3e-Zn** that was difficult to obtain by using NEt_3 as the base (Scheme 2).

The studies of the complexes by NMR revealed interesting information, most notably the effect of concentration on their formation and stability. In the ^{1}H NMR spectra of several of the complexes depicted in Scheme 5, a significant concentration dependency of the ^{1}H NMR resonances was found. The complexes of general form **3d-Zn-Base** could be divided in two categories according to how differences in concentration affected their ^{1}H NMR resonances in $CDCl_3$. In the first category of complexes (Category 1), a concentration effect on the resonances was evident. This was valid for complexes of pyridine, *N*-MeIm, TMG and DMAP. At low concentrations, resonances at higher ppm values were observed, and at high concentrations, resonances at lower ppm values were observed. This could indicate that the pentacoordinated complex is not a static assembly, and that there is an equilibrium involved between different species. Complex **3d-Zn-pyridine** is a useful model, due to the availability of $[D_5]$pyridine as a NMR solvent. From the NMR studies of **3d-Zn** in $[D_5]$pyridine, it was found that the ^{1}H NMR spectrum of **3d-Zn** did not change when changing the concentration of the complex (Scheme 6a), similar to what was observed from ^{1}H NMR studies of **4a-Zn** in $[D_6]$DMSO. Contrary observations were made when the isolated complex **3d-Zn-pyridine** was studied in $CDCl_3$. At low concentrations of the complex (2.6×10^{-3} mM), the chemical shifts were found to be relatively similar to those observed for **3d-Zn** in $CDCl_3$

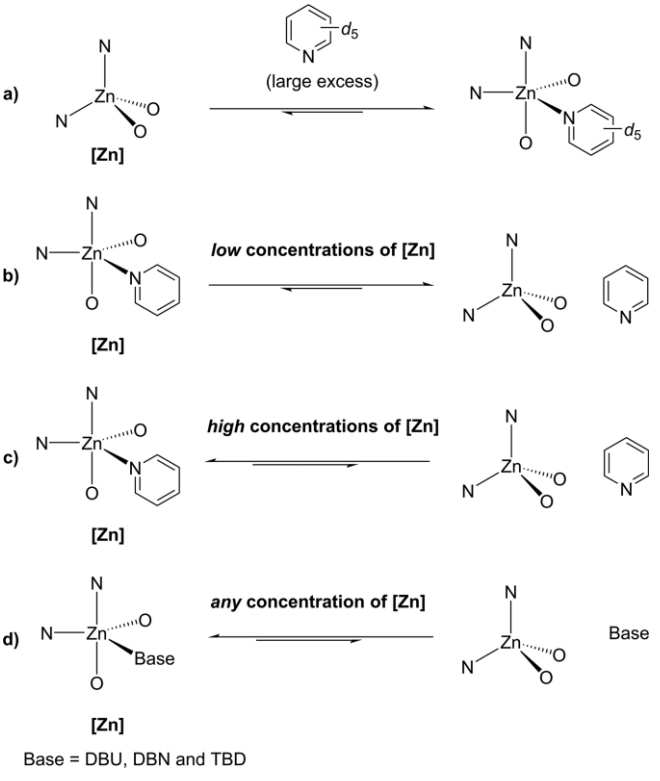

Scheme 6. Suggested effect of concentration on **3d-Zn** in $[D_5]$pyridine (a), on **3d-Zn-pyridine** in $CDCl_3$ (b) and (c), and on **3d-Zn-DBU**, **3d-Zn-DBN** and **3d-Zn-TBD** in $CDCl_3$ (d).

© 2020 The Authors published by Wiley-VCH GmbH

(Scheme 6b). Upon increasing the concentration of **3d-Zn-pyridine** (2.6×10^{-2} mM), the chemical shifts were moved to lower ppm values, the strongest effect was found for the resonance corresponding to H^a (see Figure 3) and the α-protons of pyridine, indicating a larger extent of pentacoordination in the observed species (Scheme 6c).

From the studies of the complexes, a second category of complexes **3d-Zn-Base** could be established (Category 2). The ^{1}H NMR appearance of complexes **3d-Zn-DBU**, **3d-Zn-DBN** and **3d-Zn-TBD** in $CDCl_3$ was found to be essentially independent of the concentration of the corresponding complex (Scheme 6d). This indicates that Zn in complex **3d-Zn** has a higher affinity for DBU, DBN and TBD than e.g. pyridine, which could be rationalized by the higher basicity of the former compared to the latter.[26]

As the complexes in Category 1 were dynamic in ^{1}H NMR with respect to concentration, it complicated their NMR analysis. Complexes **3d-Zn-DBU** and **3d-Zn-TBD** were more suitable for in-depth NMR studies as no concentration dependency could be detected. Although DBU and TBD are structurally similar to each other, some significant differences in the ^{1}H NMR spectra of their respective complexes were found. Broadened ^{1}H NMR resonances were observed for **3d-Zn-DBU** in $CDCl_3$ at ambient temperature, whereas decoalescence of the resonances were observed for **3d-Zn-TBD**, revealing the non-symmetrical nature of the pentacoordinated complex. Initial studies of **3d-Zn-TBD** were conducted at 25 °C, but a small temperature decrease (15 °C) made the decoalescence more evident. Studies of **3d-Zn-DBU** at the same temperature did not reveal any decoalescence, whereas complex **3d-Zn-TMG**, also carrying a guanidine ligand, had sharp ^{1}H NMR resonances at this temperature (Figure 6).

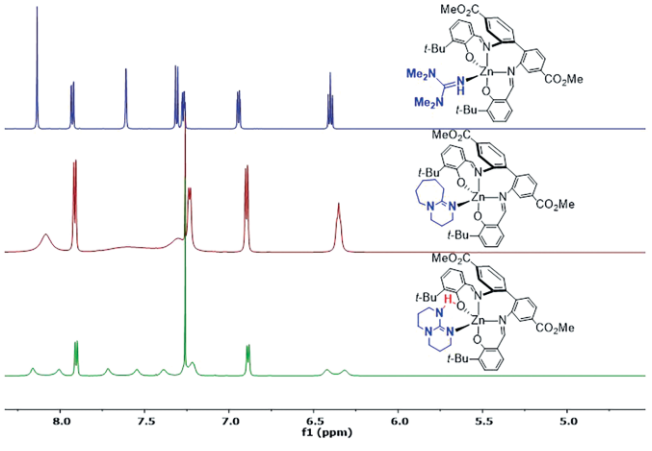

Figure 6. Stacked ^{1}H NMR (600 MHz, $CDCl_3$, 15 °C) spectra of **3d-Zn-TMG** (top), **3d-Zn-DBU** (middle) and **3d-Zn-TBD** (bottom) highlighting the significance of the N-ligand on the appearance of the ^{1}H NMR resonances of the corresponding complex. Only the aromatic region is shown.

One possible explanation for the increase in conformational stability for the TBD complex compared to the DBU complex and the TMG complex is the ability of intramolecular hydrogen-bonding in the former than the two latter complexes. The NH proton of the TBD ligand in **3d-Zn-TBD** could not be observed in $CDCl_3$, probably because of rapid H-D exchange in this solvent.[29] The resonance of the NH proton of **3d-Zn-TBD** was observed at 6.17 ppm in CD_2Cl_2, which is a significantly higher ppm value than what was found for the resonance of the NH proton of TBD in CD_2Cl_2 (4.42 ppm). Similar changes were observed in C_6D_6. This may be indicative of hydrogen-bonding in solution. In addition, data from single-crystal X-ray diffraction analysis of **3d-Zn-TBD** indicated hydrogen-bonding in solid state (vide infra). Intramolecular hydrogen bond formation in TBD complexes of various metals have been reported,[30] and Hitchcock and co-workers reported a similar change of the resonance of the NH proton in TBD in the complex $ZnBr_2(TBD)_2$ in CD_2Cl_2[30a] as to what was observed for **3d-Zn-TBD**.

More detailed variable temperature ^{1}H NMR studies of **3d-Zn-DBU** and **3d-Zn-TBD** revealed other interesting differences between these complexes. The primarily effect of additional temperature decrease for **3d-Zn-TBD** (vide infra) was a gradually sharpening of the resonances that had underwent decoalescence at 15 °C (Figure 8 and Figure S242, SI). For **3d-Zn-DBU**, decoalescence of some of the resonances was observed at 3 °C, and at −8 °C a second decoalescence process was observed. On further decreasing the temperature to −44 °C, all resonances became sharper. The process was most easily observed for the imine proton H^d (Figure 7).

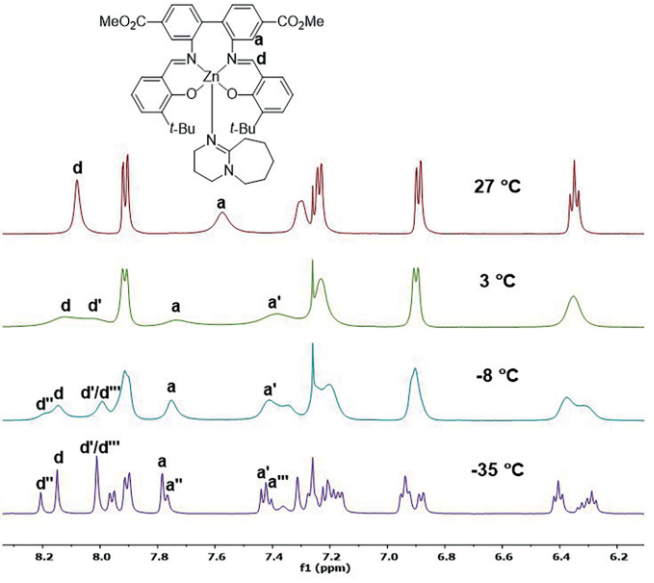

Figure 7. Stacked ^{1}H NMR (500 MHz, $CDCl_3$) spectra of **3d-Zn-DBU** on decreasing temperature. Only the aromatic region is shown.

The most reasonable explanation for the observations in Figure 7 is that in case of **3d-Zn-DBU** there are two equilibrating pentacoordinated complexes present (Scheme 7).

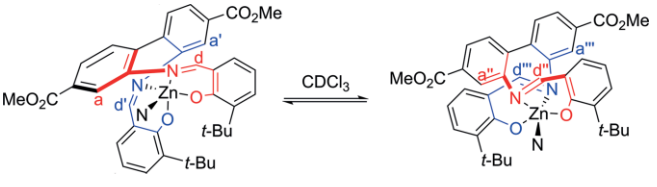

Scheme 7. Model of pseudorotation in **3d-Zn-DBU**. The DBU ligand has been omitted for clarity and is represented by "N".

© 2020 The Authors published by Wiley-VCH GmbH

Full Paper
doi.org/10.1002/ejic.202000589

This would lead to the decoalescence of proton H^d into four resonances H^d, $H^{d'}$, $H^{d''}$ and $H^{d'''}$. However, only three resonances were observed at the lowest temperature that was investigated. The ratios between the resonances $H^{d''}$, H^d and $H^{d'}$ at –44 °C in Figure 7 were found to be 0.3:0:7:1 by integration. Based on this, it would be anticipated that the resonance $H^{d'}$ actually contains two resonances $H^{d'}$ and $H^{d'''}$ in the same relative ratio as that observed within the pair $H^{d''}$ and H^d. The effect may indeed be observable for proton H^a, but unfortunately overlap with other resonances in the ^{1}H NMR spectrum make the unambiguous assignment of all four resonances H^a, $H^{a'}$, $H^{a''}$ and $H^{a'''}$ impossible.

A second explanation for the observations made for **3d-Zn-DBU** in Figure 7, may be that the dominating equilibrium for this complex is that depicted in Scheme 6d, i.e. between a pentacoordinated complex and a tetracoordinated complex. In order to investigate whether the equilibrium depicted in Scheme 6d really was operating for the DBU-ligated complex, a ^{1}H NMR experiment was performed. In an equilibrium process, a small amount of uncoordinated DBU would be present at any time. DBU is a useful strong base for numerous organic reactions,[31] such as transesterifications.[32] Importantly, it can be used catalytically in such reactions.[33] In virtue of having ethoxycarbonyl substituents, **4e-Zn-DBU** could then react with another alcohol, i.e. CD_3OD, in the presence of catalytic amounts of DBU released in solution to produce the transesterification products, **3e-CD_3-Zn-DBU** and ethanol (Scheme 8).

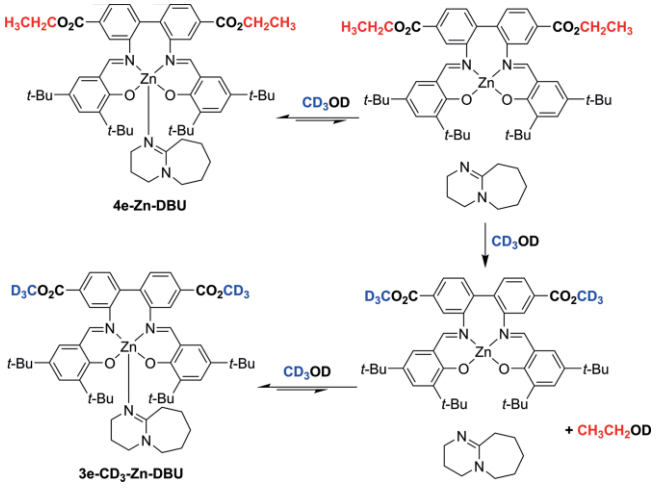

Scheme 8. Suggested formation of **3e-CD_3-Zn-DBU** from **4e-Zn-DBU** in CD_3OD.

Thus, the ^{1}H NMR spectrum of **4e-Zn-DBU** in CD_3OD was recorded. Initially a small amount of ethanol could be detected alongside the resonances belonging to the ethoxycarbonyl group, and after one day, there were only traces left of the ethoxycarbonyl group, alongside an increased amount of ethanol (Figure S359, SI). The presence of the deuterated complex **3e-CD_3-Zn-DBU** was verified by MS. These observations suggest that there indeed is an equilibrium involved for the DBU-ligated complexes, between a pentacoordinated and a tetracoordinated species. Furthermore, the transesterification did not take place when **4e-Zn** was studied in CD_3OD under similar conditions, indicating that DBU is needed for the reaction to take place.

Whereas the equilibrium between a pentacoordinated complex and a tetracoordinated complex could not be directly observed from the variable temperature NMR studies of **3d-Zn-DBU**, it was possible to detect it from the studies of **3d-Zn-TBD** (Figure 8).

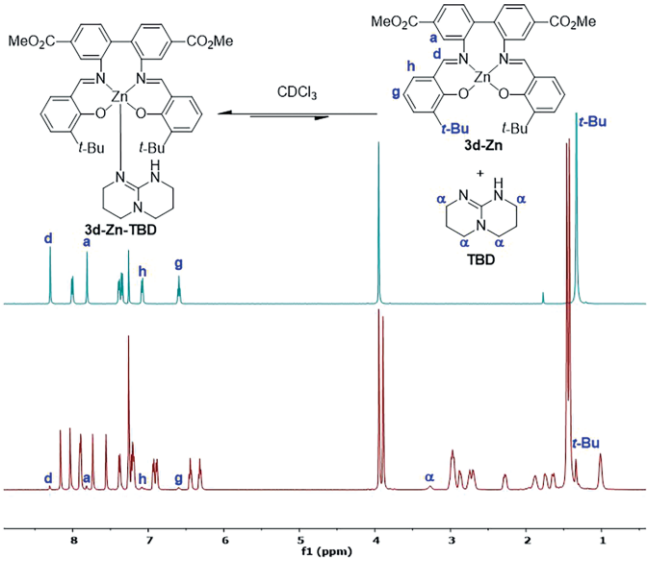

Figure 8. Stacked ^{1}H NMR (500 MHz, $CDCl_3$, –44 °C) of **3d-Zn** (top) and **3d-Zn-TBD** (bottom), showing the coexistence of the two complexes in the bottom spectrum.

Unlike what was observed for **3d-Zn-DBU**, no secondary decoalescence process could be observed for **3d-Zn-TBD**, which may be attributed to the ability of intramolecular hydrogen-bonding in the complex as discussed above. However, at sufficiently low temperatures (≤ –22 °C), the resonances belonging to a second species were revealed, which is most probably the tetracoordinated species **3d-Zn** from comparisons with the ^{1}H NMR spectrum of the latter at the same temperatures. Furthermore, additional resonances in the aliphatic region of the ^{1}H NMR spectrum of **3d-Zn-TBD** could be attributed to uncoordinated TBD. The ratio between **3d-Zn-TBD** and **3d-Zn** was estimated to be 1:0.04 from integration of the ^{1}H NMR spectrum of **3d-Zn-TBD**, which is in agreement with the proposal in Scheme 6d, with the equilibrium being strongly in favor of the pentacoordinated complex, at least at low temperatures. In addition to **3d-Zn-DBU** and **3d-Zn-TBD**, a third complex, **3d-Zn-DMAP** was studied using variable temperature ^{1}H NMR. As opposed to the two former complexes, the ^{1}H NMR resonances of the latter complex were sharp at room temperature, similar to what was observed for **3d-Zn-TMG** (upper spectrum, Figure 6). On decreasing the temperature to –56 °C, the ^{1}H NMR resonances of **3d-Zn-DMAP** became broadened, but the decoalescence temperature could not be reached in $CDCl_3$ (Figure S259, SI).

In addition to the studies conducted on base-ligated complexes of **3d-Zn**, **3e-Zn** and **4e-Zn**, a series of other base-ligated complexes were synthesized, using the reaction conditions described in Scheme 5a. On comparison of the *ortho-tert*-butyl-substituted complex **3d-Zn-DBU** and the *ortho*-fluorine-substi-

© 2020 The Authors published by Wiley-VCH GmbH

Full Paper
doi.org/10.1002/ejic.202000589

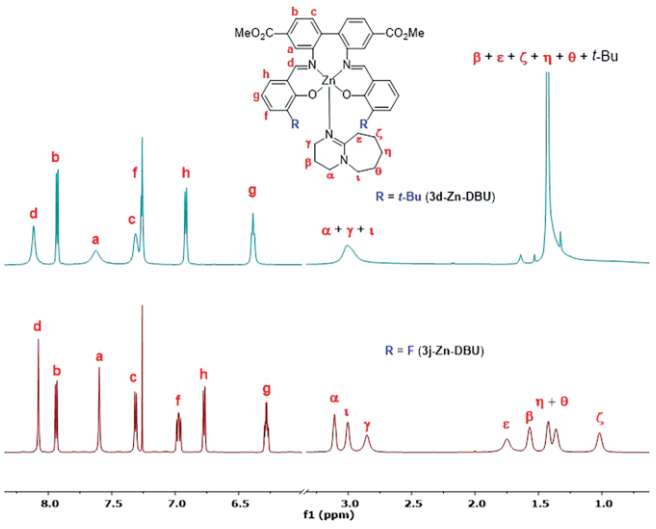

Figure 9. Stacked ^{1}H NMR (600 MHz, $CDCl_3$, 25 °C) spectra of **3d-Zn-DBU** (top) and **3j-Zn-DBU** (bottom) showing the aromatic and the aliphatic region.

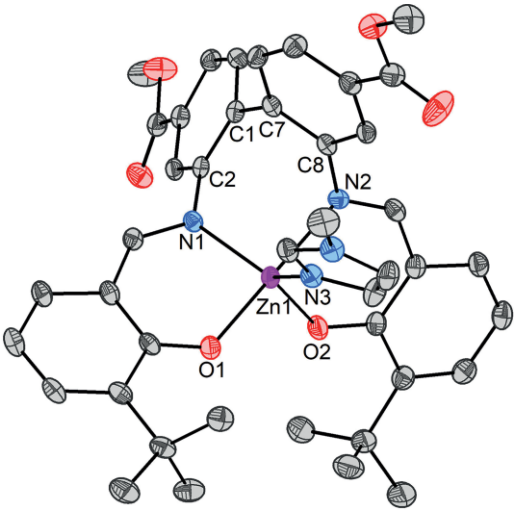

Figure 10. ORTEP plot of **3d-Zn-N-MeIm** with 50 % ellipsoids. Hydrogen atoms have been omitted for clarity. τ_5 = 0.83. Selected bond lengths [Å] and angles [°]: Zn1–N1, 2.0712(1); Zn1–N2, 2.1901(1); Zn1–N3, 2.0751(1); Zn1–O1, 1.9834(1); Zn1–O2, 1.9372(1); N1–Zn1–N2, 91.315(2); N1–Zn1–N3, 125.842(3); N1–Zn1–O1, 90.391(3); N1–Zn1–O2, 118.977(3); N2–Zn1–N3, 84.573(2); N2–Zn1–O1, 175.708(3); N2–Zn1–O2, 86.425(3); N3–Zn1–O1, 91.236(3); N3–Zn1–O2, 114.617(3); O1–Zn1–O2, 96.190(3); C2–C1–C7–C8, 65.639(7).

tuted complex **3j-Zn-DBU**, significant differences in the ^{1}H NMR spectra of the two complexes were found (Figure 9).

Both the resonances belonging to the DBU ligand and the aromatic resonances were significantly sharper and more well-defined for **3j-Zn-DBU** than for **3d-Zn-DBU**. This may indicate that not only the size of the *N*-ligand, but also the steric and electronic properties of the N_2O_2 ligand are crucial for the isomerization rates of the pentacoordinated Zn complexes described herein.

Although NMR proved to be very useful for the studies of the interactions between the Zn complexes and the different Lewis bases described herein, attempts to study the Zn complexes and their interactions with other Lewis bases (halide anions) were less conclusive. Only very subtle changes in the ^{1}H NMR resonances of the complexes **3d-Zn** and **4d-Zn** in $CDCl_3$ could be observed on addition of tetrabutylammonium halide salts. The ^{1}H NMR studies of **3d-Zn** and **4d-Zn** in the presence of tetrabutylammonium cyanide in $CDCl_3$ were complicated by coinciding decomposition of the complexes. The coordination of water to complex **3j-Zn** could be detected by ^{1}H NMR, but only in $CDCl_3$ (see S154, SI).

Crystallographic Structure Determination of Base-Ligated Pentacoordinated Zn Complexes

Complexes **3d-Zn-*N*-MeIm**, **3e-Zn-DMAP**, **4e-Zn-DBU**, **3d-Zn-TBD** and **3e-Zn-TMG** (Figure 10, Figure 11, Figure 12, Figure 13, and Figure 14) were characterized by single-crystal X-ray diffraction analysis.

All five complexes crystallized with the anticipated pentacoordination around Zn, with distorted trigonal bipyramidal geometries as evaluated by the τ_5 values[34] of the structures. The obtained structures clearly show that the salicylaldiminato half-units within each complex do not have an identical environment, thus explaining the observations made in the ^{1}H NMR spectra of **3d-Zn-TBD** and **3e-Zn-DBU**. On comparison of the bond lengths between Zn and the nitrogen of the different

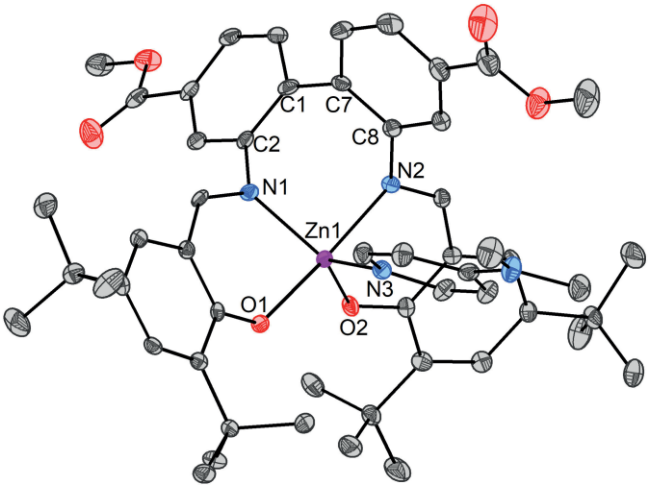

Figure 11. ORTEP plot of **3e-Zn-DMAP** with 50 % ellipsoids. Only one of the two molecules in the asymmetric unit is shown. Hydrogen atoms have been omitted for clarity. τ_5 = 0.89, 0.89. Selected bond lengths [Å] and angles [°]: Zn1–N1, 2.0711(1); Zn1–N2, 2.1563(1); Zn1–N3, 2.0936(1); Zn1–O1, 1.9919(2); Zn1–O2, 1.9358(1); Zn2–N4, 2.1630(1); Zn2–N5, 2.0723(1); Zn2–N6, 2.0949(1); Zn2–O3, 1.9294(2); Zn2–O4, 1.9942(1); N1–Zn1–N2, 89.722(3); N1–Zn1–N3, 119.986(4), N1–Zn1–O1, 87.220(3); N1–Zn1–O2, 122.369(3); N2–Zn1–N3, 87.468(3); N2–Zn1–O1,176.065(4); N2–Zn1–O2, 86.752(3); N3–Zn1–O1, 91.915(4); N3–Zn1–O2, 117.282(3); O1–Zn1–O2, 96.977(3); C2–C1–C7–C8, 61.396(8); N4–Zn2–N5, 90.028(3); N4–Zn2–N6, 86.413(3), N4–Zn2–O3, 86.776(3); N4–Zn2–O4, 176.305(4); N5–Zn2–N6, 118.997(4); N5–Zn2–O3,123.184(3); N5–Zn2–O4, 87.601(3); N6–Zn2–O3, 117.368(3); N6–Zn2–O4, 92.257(4); O3–Zn2–O4, 96.894(3).

base ligands, the bond lengths were found to range from 2.0444(1) Å to 2.0936(1) Å. From the categorization of complexes based on their behavior towards concentration effects in solution, it would be anticipated that for complexes belonging to the first category (**3d-Zn-*N*-MeIm**, **3e-Zn-DMAP** and **3e-Zn-**

© 2020 The Authors published by Wiley-VCH GmbH

Full Paper
doi.org/10.1002/ejic.202000589

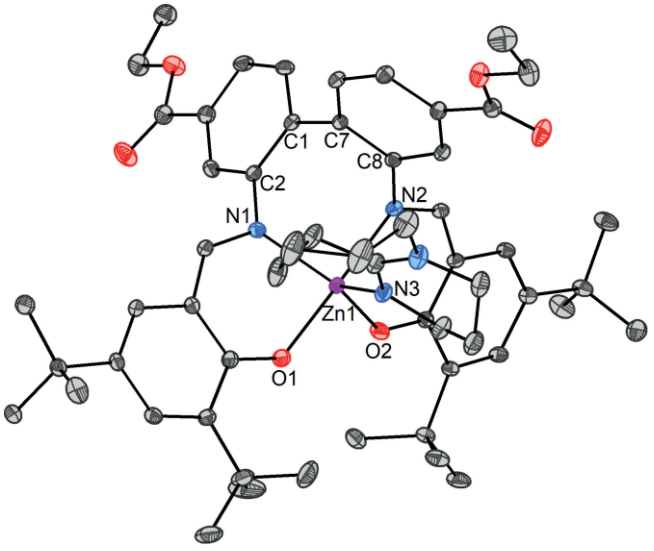

Figure 12. ORTEP plot of **4e-Zn-DBU** with 50 % ellipsoids. Hydrogen atoms have been omitted for clarity. τ_5 = 0.72. Selected bond lengths [Å] and angles [°]: Zn1–N1, 2.0974(1); Zn1–N2, 2.1512(1); Zn1–N3, 2.0883(1); Zn1–O1, 1.9815(1); Zn1–O2, 1.9659(1); N1–Zn1–N2, 90.649(3); N1–Zn1–N3, 119.402(3); N1–Zn1–O1, 88.015(3); N1–Zn1–O2, 128.793(3); N2–Zn–N3, 90.723(3); N2–Zn1–O1, 171.865(3); N2–Zn1–O2, 85.620(3); N3–Zn1–O1, 96.925(3); N3–Zn1–O2, 111.708(4); O1–Zn1–O2, 88.964(3); C2–C1–C7–C8, 67.082(7).

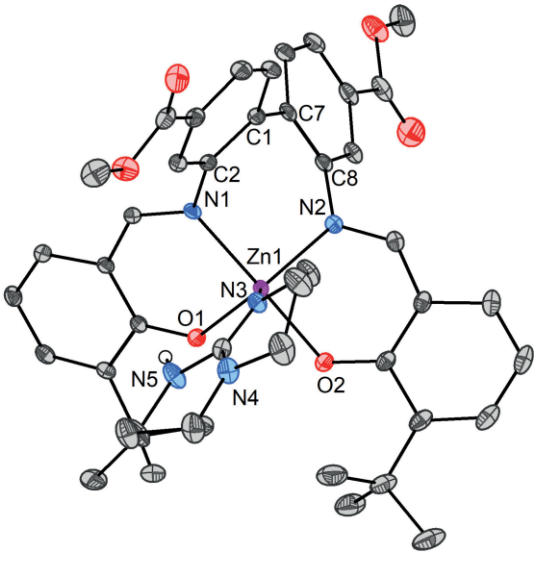

Figure 13. ORTEP plot of **3d-Zn-TBD** with 50 % ellipsoids. Hydrogen atoms (except N5–H) have been omitted for clarity. τ_5 = 0.71. Selected bond lengths [Å] and angles [°]: Zn1–N1, 2.1304(1); Zn1–N2, 2.0874(1); Zn1–N3, 2.0559(1); Zn1–O1, 1.9701(1); Zn1–O2, 2.0204(1); N5···O1, 2.9841(1); N1–Zn1–N2, 90.618(3); N1–Zn1–N3, 93.411(3); N1–Zn1–O1, 87.268(3); N1–Zn1–O2, 174.622(3); N2–Zn1–N3, 90.618(3); N2–Zn1–O1, 131.876(3); N2–Zn1–O2, 88.793(3); N3–Zn1–O1, 114.969(3); N3–Zn1–O2, 91.736(3); O1–Zn1–O2, 89.145(3); C2–C1–C7–C8, –60.396(7); N5–H···O1, 147.413(5).

TMG), the Zn-N(base) bonds would be longer than for complexes belonging to the second category (**4e-Zn-DBU** and **3d-Zn-TBD**). However, there was no clear correlation between these observations and the obtained bond lengths. The Zn-N bond lengths were found to increase in the order **3e-Zn-TMG** < **3d-Zn-TBD** < **3d-Zn-*N*-MeIm** < **4e-Zn-DBU** < **3e-Zn-DMAP**.

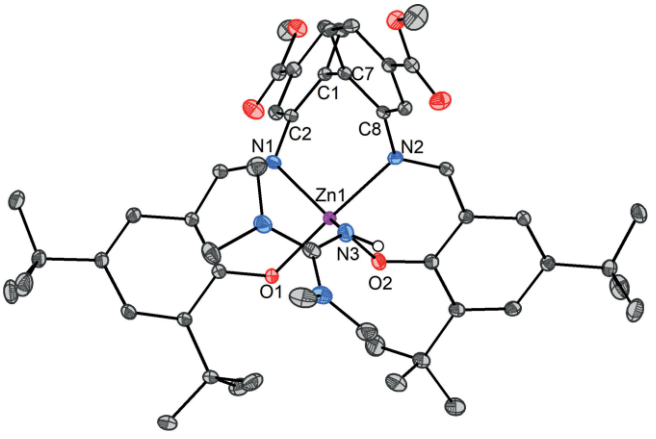

Figure 14. ORTEP plot of **3e-Zn-TMG** with 50 % ellipsoids. Hydrogen atoms (except for N3–H) and MeCN (solvent of crystallization) have been omitted for clarity. τ_5 = 0.77. Selected bond lengths [Å] and angles [°]: Zn1–N1, 2.0869(1); Zn1–N2, 2.1699(1); Zn1–N3, 2.0444(1); Zn1–O1, 2.0042(1); Zn1–O2, 1.9524(1); N3···O1, 3.0357(2); N3···O2, 3.2834(1); N1–Zn1–N2, 92.200(3); N1–Zn1–N3, 127.099(3); N1–Zn1–O1, 87.435(3); N1–Zn1–O2, 122.323(4); N2–Zn1–N3, 88.613(3); N2–Zn1–O1, 173.053(4); N2–Zn1–O2, 85.121(3); N3–Zn1–O1, 97.144(3); N3–Zn1–O2, 110.453(3); O1–Zn1–O2, 89.211(3); C2–C1–C7–C8, 68.579(8); N3–H···O1, 48.341(5); N3–H···O2, 86.435(5).

Since the obtained structures have varied deviations from ideal trigonal bipyramidal geometry, this must be taken into consideration when comparing the data. Another perspective could be obtained by comparing the three different Zn-N bonds within each complex. For **3d-Zn-*N*-MeIm** and **3e-Zn-DMAP**, the shortest bond is between Zn and one of the N donors in the N_2O_2 ligand. For the three other complexes, the shortest bond is between Zn and the N donor of the base ligand. This may account for the differences in stability observed for **3d-Zn-*N*-MeIm** and **3e-Zn-DMAP**, and **3d-Zn-TBD** and **4e-Zn-DBU** in solution, although **3e-Zn-TMG** does not fit in this pattern, based upon both bond lengths and basicity of the ligand itself. Hence, it is clear that other factors are important as well, e.g. the size of the ligand as well as secondary stabilizing interactions between the different complexes in solution.[5b] Intramolecular hydrogen-bonding within **3d-Zn-TBD** was discussed as a possible explanation for the increased conformational stability for this complex compared to e.g. **3d-Zn-DBU** and **3d-Zn-TMG**. Both the donor–acceptor bond length and the hydrogen bond angle within **3d-Zn-TBD** are within the range of hydrogen-bonding of moderate strength,[35] and these values support the assumptions made from the ^{1}H NMR data. No clear indications of intramolecular hydrogen-bonding were found for **3e-Zn-TMG** in the solid state, although this complex also have an NH-containing guanidine ligand. This observation is in accordance with the literature reports concerning the coordination chemistry of guanidines, as bicyclic guanidines (e.g. TBD) have a greater tendency to participate in intramolecular hydrogen bonding than acyclic guanidines (e.g. TMG).[30b,36]

Synthesis, NMR Studies and Single-Crystal X-ray Diffraction Analysis of Cd Complexes 4b-Cd, 4a-Cd-DBU and 4e-Cd-DBU

In addition to the studies on Zn, preliminary studies were conducted on Cd as well. This was of special interest as Zn and Cd

© 2020 The Authors published by Wiley-VCH GmbH

Full Paper
doi.org/10.1002/ejic.202000589

have many similarities in terms of coordination chemistry.[37] The main difference between Zn and Cd is the larger ionic radius of the latter than the former.[38] Cd is also considered to be a softer Lewis acid than Zn.[39] Both these factors should be of relevance for studies of metal complexes of the N_2O_2 tetradentate ligands described herein. Initially, when ligand **4a** was treated with $Cd(OAc)_2{\cdot}2H_2O$ or $CdCl_2$ using the same reaction conditions as those for the synthesis of the Zn complex **4a-Zn**, only a product of low purity could be obtained. Similar results were obtained using ligand **4e**, and no Cd complex could be isolated from the reaction. However, better results were obtained using the more electron poor ligand **4b**, and the corresponding Cd complex **4b-Cd** could be obtained in moderate yields using the reaction conditions depicted in Scheme 9.

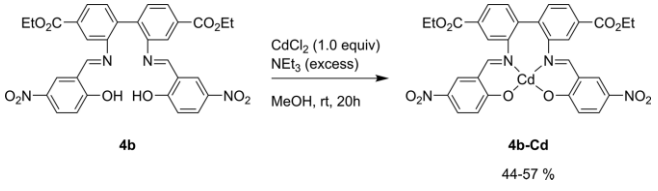

Scheme 9. Synthesis of Cd complex **4b-Cd**.

The Cd complex was characterized by NMR spectroscopy, MS, elemental analysis and single-crystal X-ray diffraction analysis. Crystals suitable for single-crystal X-ray diffraction analysis was obtained by slow diffusion of methanol into a saturated solution of **4b-Cd** in DMSO, giving **4b-Cd-DMSO-MeOH**. The complex crystallized as a monomer with distorted octahedral geometry around Cd. The N_2O_2 ligand occupied four of the six coordination sites, whereas the two last sites were occupied by a DMSO molecule and a MeOH molecule (Figure 15).

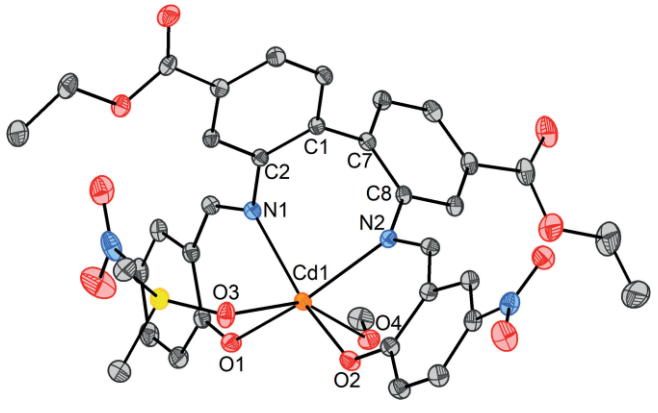

Figure 15. ORTEP plot of **4b-Cd-DMSO-MeOH** with 50 % ellipsoids. Hydrogen atoms have been omitted for clarity. Selected bond lengths [Å] and angles [°]: Cd1–N1, 2.3435(1); Cd1–N2, 2.3224(1); Cd1–O1, 2.2579(1); Cd1–O2, 2.2120(1); Cd1–O3, 2.3186(1); Cd1–O4, 2.3737(1); N1–Cd1–N2; 86.043(1); N1–Cd1–O1, 80.174(1); N1–Cd1–O2, 153.388(2); N1–Cd1–O3, 88.640(1); N1–Cd1–O4, 110.812(2); N2–Cd1–O1, 150.990(2); N2–Cd1–O2, 81.709(1); N2–Cd1–O3, 121.794(2); N2–Cd1–O4, 80.941(1); O1–Cd1–O2, 120.355(2); O1–Cd1–O3, 83.486(2); O1–Cd1–O4, 80.331(2); O2–Cd1–O3, 78.083(2); O2–Cd1–O4, 90.525(2); O3–Cd1–O4, 151.924(2); C2–C1–C7–C8, –75.114(4).

The octahedral geometry found for **4b-Cd-DMSO-MeOH** can best be described as severely distorted. The Cd–N and Cd–O bonds between Cd and the Schiff base ligand are of comparable length to reported values for hexacoordinated Cd Schiff base complexes.[40] The *trans* angles in the complex were found to be 153.388(2)°, 150.990(2)° and 151.942(2)° for N1–Cd1–O2, N2–Cd1–O1 and O3–Cd1–O4 respectively, showing large deviations from the expected 180° angles. The *cis* angles were also deviating from the expected 90° angles, ranging between 78.083(2) and 121.794(2)°. There are several reports of hexacoordinated Cd complexes of multidentate ligands with strongly distorted octahedral geometry,[40a,41] and even trigonal prismatic geometry[42] in the literature, creating a clear precedence for the distorted geometry observed for **4b-Cd-DMSO-MeOH**.

The effect of increased ionic radius for Cd compared to Zn can be seen by the enhancement of coordination number of the Cd complex, together with the elongation of all the bonds between the metal ion and the heteroatoms of the N_2O_2 ligand. Although Cd is considered to be a softer Lewis acid than Zn, the DMSO ligand coordinates via oxygen and not sulfur,[43] and oxygen coordination in Cd-DMSO complexes is frequently reported in the literature.[44] The pseudo-octahedral geometry found for **4b-Cd-DMSO-MeOH** may explain the low stability of the complex in other NMR solvents than [D_6]DMSO. Whereas the Zn complexes described herein could be studied in different solvents, **4b-Cd** was found to decompose rapidly in $CDCl_3$ and even in CD_3CN, thus limiting NMR studies to [D_6]DMSO. Cd coordination was readily detected by ^{1}H NMR spectroscopy, and Cd satellites were visible for the imine proton in **4b-Cd** with $^3J_{H,Cd}$ of 26.8 Hz. The value is comparable with what has previously been reported for Schiff base complexes of Cd.[42c,45] Cd satellites were also observed in the ^{13}C NMR spectrum of the complex, but only three-bond coupling constants could be detected, and only for carbons in the phenoxide rings of the complex. $^3J_{C,Cd}$ values for C^{10} and C^8 were found to be 15.0 Hz and 21.0 Hz, respectively (Figure 16). These coupling constants are comparable with reported values in the literature for Schiff base complexes of Cd.[46]

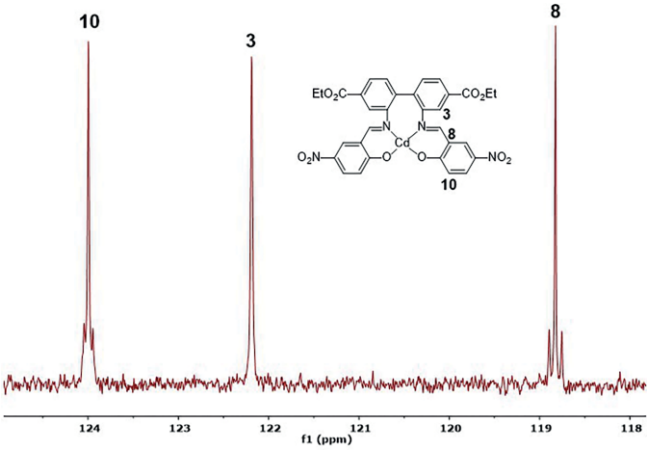

Figure 16. Excerpt of the ^{13}C NMR (151 MHz, [D_6]DMSO) spectrum of **4b-Cd** showing the resonances corresponding to C^{10}, C^3 and C^8 (left to right). Only C^{10} and C^8 show coupling to Cd, although C^3 also would be expected to have a ^3J coupling to Cd.

The significantly longer Cd–N bonds in the complex, compared to the Cd–O bonds, may explain the lack of observed ^3J coupling between Cd and C^3 (see Figure 16). The weak nature of the Cd–N bonds could also be observed in ^{1}H-^{15}N HMBC

© 2020 The Authors published by Wiley-VCH GmbH

experiments. The coordination shift $\Delta\delta$ ($\delta_{complex} - \delta_{ligand}$) of the imine nitrogen was less in **4b-Cd** ($\Delta\delta$ = 18.1) than in **4b-Zn** ($\Delta\delta$ = 33.5) on comparison with that of ligand **4b**.

Whereas ligands **4a** and **4e** failed to yield Cd complexes when the reactions was carried out in the presence of NEt_3, Cd complexes of these ligands could be obtained when DBU was used as the base. As was found for Zn, DBU-ligated complexes were obtained in moderate to good yields (Scheme 10).

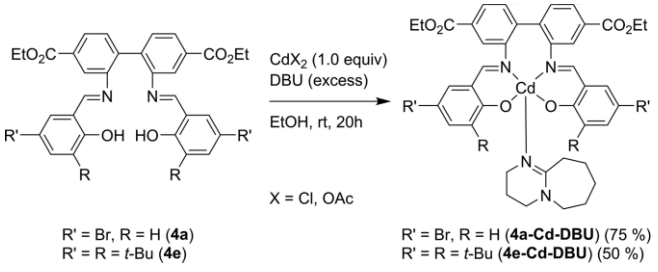

Scheme 10. Synthesis of Cd complex **4b-Cd**.

The complexes were characterized by NMR spectroscopy, MS, elemental analysis and single-crystal X-ray diffraction analysis. **4e-Cd-DBU** crystallized as a monomer with pentacoordination at Cd, analogously to what was seen for the corresponding Zn complex (Figure 17).

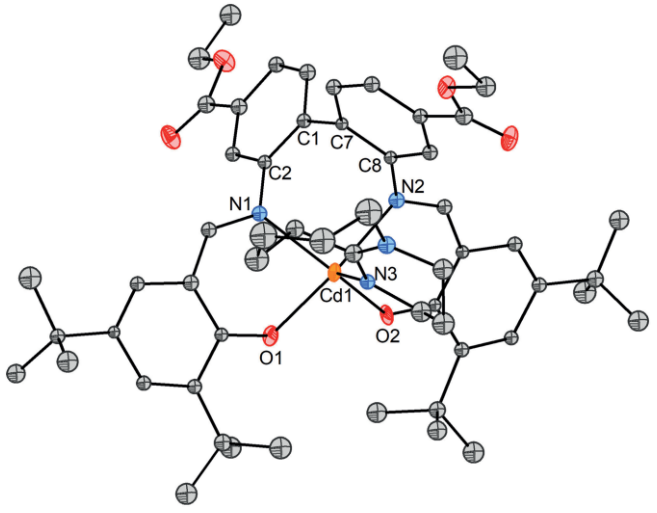

Figure 17. ORTEP plot of **4e-Cd-DBU**. Because of disorder limiting the high-resolution diffraction in the measured crystal, only Zn and O are refined as thermal ellipsoids (set at 50 % probability). Hydrogen atoms have been omitted for clarity. τ_5 = 0.52. Selected bond lengths [Å] and angles [°]: Cd1–N1, 2.2876(2); Cd1–N2, 2.3158(2); Cd1–N3, 2.2634(3); Cd1–O1, 2.1468(2); Cd1–O2, 2.1595(2); N1–Cd1–N2, 90.609(6); N1–Cd1–N3, 118.298(6); N1–Cd1–O1, 81.832(5); N1–Cd1–O2, 128.766(6); N2–Cd1–N3, 93.208(5); N2–Cd1–O1, 159.802(6); N2–Cd1–O2, 80.252(5); N3–Cd1–O1, 106.881(6); N3–Cd1–O2, 112.514(7); O1–Cd1–O2, 89.894(6); C2–C1–C7–C8, 77.236(15).

Whereas **4e-Zn-DBU** crystallized with distorted trigonal bipyramidal geometry around Zn (τ_5 = 0.72), the geometry around Cd in **4e-Cd-DBU** was found to be intermediate between trigonal bipyramidal and square pyramidal (τ_5 = 0.52). Of the three Cd–N bonds, the bond between Cd and the DBU ligand (2.2634(3) Å) was shorter than the corresponding bonds between Cd and the N_2O_2 ligand (2.3158(2) Å and 2.2876(2) Å, respectively). On comparison with the Zn complex **4e-Zn-DBU** (Figure 12), the bond between Cd and the DBU ligand was significantly longer than the corresponding bond between Zn and DBU (2.0883(1) Å).

As was seen for **4b-Cd**, coordination of Cd in **4e-Cd-DBU** could be detected by the presence of Cd satellites in both ^{1}H and ^{13}C NMR. While **4b-Cd** only could be characterized in [D_6]DMSO due to stability issues, **4e-Cd-DBU** was more robust towards degradation in solution. Although most NMR characterization of the Cd complex was performed in [D_6]DMSO, some characterization could also be carried out in $CDCl_3$, although degradation of the complex took place over time. This suggest that the preferred coordination number of the Cd complex in solution would be six, and that the pentacoordinated species (presumably present in $CDCl_3$) is less stable than a hexacoordinated species (presumably present in [D_6]DMSO).

The ^{1}H NMR spectrum of **4a-Cd-DBU** was similar to that of **4e-Cd-DBU**, with the expected 1:1 stoichiometry between the N_2O_2 ligand and the DBU ligand. The spatial proximity of the different ligands at Cd was established by ^{1}H-^{1}H NOESY experiments. **4a-Cd-DBU** was characterized by single-crystal X-ray diffraction analysis as well, showing strikingly different results than those obtained for **4e-Cd-DBU**. Crystals were obtained by slow diffusion of EtOH into a saturated DMSO solution of **4a-Cd-DBU**. The complex crystallized as a tetramer, with each of the four Cd nuclei having a distorted octahedral geometry (Figure 18 and Figure 19). Furthermore, the complex crystallized without *any* DBU ligands, and the coordination environment was solely made up by four molecules of the N_2O_2 ligand.

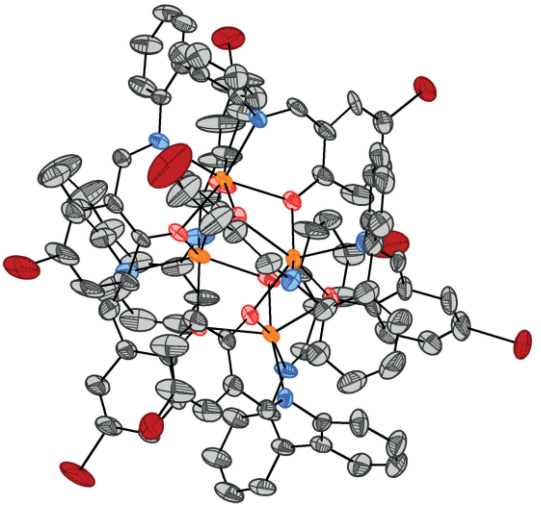

Figure 18. ORTEP plot of **4a-Cd** with 50 % ellipsoids. Hydrogen atoms and ethoxycarbonyl groups have been omitted for clarity.

As seen from Figure 18 and Figure 19, the four Cd nuclei are interconnected by bridging oxygens, creating a cavity in the structure. The distance between the diagonally oriented Cd nuclei in this cavity was found to be 4.8074(1) Å (Cd1···Cd3) and 5.1232(1) Å (Cd2···Cd4) respectively. The bonding distances between Cd and each of the six heteroatoms were similar to those seen for the monomer **4b-Cd**, with Cd–N bond lengths ranging between 2.3109(1) Å and 2.3416(1) Å, and Cd–O bond lengths ranging between 2.2057(1) Å and 2.3762(1) Å. Although the hexacoordination observed for **4a-Cd** and **4b-Cd** was not seen

© 2020 The Authors published by Wiley-VCH GmbH

Full Paper
doi.org/10.1002/ejic.202000589

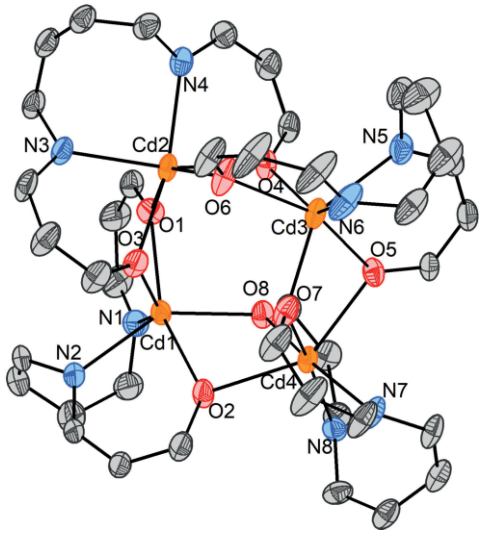

Figure 19. ORTEP plot of **4a-Cd** with 50 % ellipsoids. Only the heteroatoms coordinating to Cd, as well as the carbon atoms that connect the aforementioned heteroatoms, are shown. Selected bond lengths [Å] and angles [°]: Cd1–N1, 2.3416(1); Cd1–N2, 2.3186(1); Cd1–O1, 2.2800(1); Cd1–O2, 2.3061(1); Cd1–O3, 2.2632(1); Cd1–O8, 2.2642(1); Cd2–N3, 2.3229(1); Cd2–N4, 2.3109(1); Cd2–O1, 2.3663(1); Cd2–O3, 2.2115(1); Cd2–O4, 2.2057(1); Cd2–O6, 2.3762(1); Cd1···Cd2, 3.5008(1); Cd1···Cd3, 4.8074(1); Cd1···Cd4, 3.5468(1); Cd2···Cd4, 5.1232(1); N1–Cd1–N2, 80.107(2); N1–Cd1–O1, 79.786(1); N1–Cd1–O2, 121.236(2); N1–Cd1–O3, 144.119(2); N1–Cd1–O8, 90.198(2); N2–Cd1–O1, 120.085(2); N2–Cd1–O2, 80.797(2); N2–Cd1–O3, 90.802(1); N2–Cd1–O8, 142.569(2); O1–Cd1–O2, 154.234(2); O1–Cd1–O3, 75.015(2); O1–Cd1–O8, 93.069(2); O2–Cd1–O3, 90.864(2); O2–Cd1–O8, 73.605(2); O3–Cd1–O8, 116.018(2); N3–Cd2–N4, 88.491(2); N3–Cd2–O1, 90.433(2); N3–Cd2–O3, 79.799(2); N3–Cd2–O4, 166.549(2); N3–Cd2–O6, 115.367(2); N4–Cd2–O1, 113.098(1); N4–Cd2–O3, 113.098(1); N4–Cd2–O4, 80.701(2); N4–Cd2–O6, 92.009(2); O1–Cd2–O3, 74.268(2); O1–Cd2–O4, 85.512(2); O1–Cd2–O6, 144.914(2); O3–Cd2–O4, 111.824(2); O3–Cd2–O6, 86.788(1); O4–Cd2–O6, 73.288(2); Cd1–O1–Cd2, 97.765(1); Cd1–O3–Cd2, 102.947(1); Cd1–O2–Cd4, 98.477(2); Cd1–O8–Cd4, 105.017(2).

for any of the Zn complexes described herein, the obtained structure of **4a-Cd** may shed light on potential oligomeric structures of Zn complexes as well.

Conclusions

Herein, various Zn complexes of Schiff base ligands derived from 2,2′-diaminobiphenyls and substituted salicylaldehydes were synthesized and studied. Special emphasis was put on their behavior in solution of donating ([D_6]DMSO) and non-donating ($CDCl_3$) solvents. In $CDCl_3$, the obtained NMR data suggests that the complexes undergo a concentration dependent dimerization/oligomerization, when the steric bulk of the ligands are low. For more sterically demanding ligands, the complexes seem to exist as one species independent of concentration, presumably as tetracoordinated species. A monomeric tetracoordinated Zn complex was also structurally characterized, implying that the existence of these are much more pronounced than what has earlier been shown for the related Zn salen and salphen complexes. This may be attributed to the flexible nature of the 2,2′-diaminobiphenyl backbone of the Zn complexes herein, which allows for a possible equilibrium between a tetracoordinated and a pentacoordinated species in solution. In addition, the complexes differ from salen complexes derived from chiral diamino backbones (e.g. *trans*-1,2-diaminocyclohexane). In these complexes, Zn is tetracoordinated, but not monomeric.. Secondly, a series of Zn complexes with external nitrogen ligands were synthesized and studied. A variety of different ligands was studied, and the obtained complexes showed large variation with respect to stability in solution. For complexes of e.g. pyridine, DMAP and *N*-MeIm, the presence of pentacoordinated species were found to be strongly dependent on concentration, indicating a reversible coordination/de-coordination process. For complexes of e.g. DBU and TBD, the obtained species seemed more stable, although there were indications of a reversible process here as well. For the DBU-ligated complexes this could only be observed indirectly, but for the TBD-ligated complexes both the pentacoordinated complex and the corresponding tetracoordinated complex could be observed in ^{1}H NMR at low temperatures (≤ −22 °C). In addition to the work on the Zn complexes, Cd complexes of some of the ligands were prepared and structurally characterized, and comparisons with the aforementioned Zn complexes were made, illustrating both the similarities and differences between these two metals that are often discussed in parallel.

Experimental Section

General considerations. All chemicals were used as received. Starting materials **1b** (dimethyl 2,2′-dinitrobiphenyl-4,4′-dicarboxylate) and **2c** (ethyl 4-bromo-2-nitrobenzoate) were synthesized as described elsewhere.[8h] DMF and CH_2Cl_2 were dried using a MB SPS-800 solvent purifier system from MBraun. Other solvents were used as received. NMR spectroscopy was performed using Bruker Avance AVII400, AVIIIHD400, DRX500, AVI600, AVII600 or AVIIHD800 operating at 400 MHz (^{1}H NMR), 376 MHz (^{19}F NMR), 101 MHz (^{13}C NMR), or 500 MHz (^{1}H NMR), or 600 MHz (^{1}H NMR) and 151 MHz (^{13}C NMR), or 800 MHz (^{1}H NMR) and 201 MHz (^{13}C NMR) respectively. All spectra were recorded at room temperature unless otherwise mentioned. The temperature in the variable temperature NMR experiments were measured indirectly, by correlation of the observed probe temperature to independently measured temperatures using a Delta OHM HD9214 thermometer fitted into a NMR tube containing CD_3OD. Because of this, small deviations in the exact temperature cannot be excluded. ^{1}H NMR and ^{13}C NMR spectra have been referenced relative to the residual solvent signals, and the peaks are numbered according to Figure 20. Chemical shifts in ^{19}F NMR have been referenced to $CFCl_3$ by using C_6F_6 (–164.9 ppm with respect to $CFCl_3$ at 0 ppm) as an internal standard, and are proton decoupled. Chemical shifts in ^{15}N NMR have been calibrated against CH_3NO_2 as an external standard (0.0 ppm). All ^{15}N NMR chemical shifts were

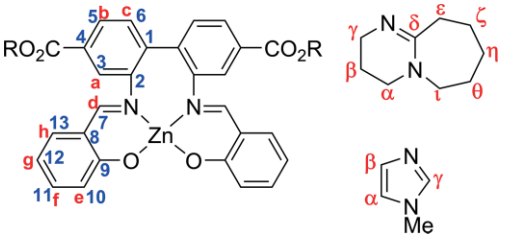

Figure 20. Numbering scheme used for reporting the NMR data. Roman letters = protons, numbers = carbons, Greek letters = protons and carbons.

© 2020 The Authors published by Wiley-VCH GmbH

obtained and assigned using ^{1}H-^{15}N HMBC experiments. The peaks in the ^{1}H NMR and ^{13}C NMR spectra were assigned using various 2D experiments (NOESY, COSY, TOCSY, HSQC, HMBC and HETCOR). MS (ESI) was recorded on a Bruker maXis II ETD spectrometer by Osamu Sekiguchi. IR spectra were recorded on a Perkin Elmer Spectrum One FT-IR spectrometer. All melting points are uncorrected and were obtained with a Stuart SMP10 melting point apparatus. Elemental analysis of selected complexes was performed by Mikroanalytisches Laboratorium Kolbe, Oberhausen, Germany. For the complexes not characterized by elemental analysis, the presence of NMR silent impurities cannot be excluded. Homogenous NMR samples were always used when assessing the purity by NMR.

X-ray Crystallography

Single crystal diffraction data were acquired on a Bruker D8 Venture equipped with a Photon 100 detector by using Mo K_α radiation (λ = 0.71073 Å) from an Incoatec iμS microsource. Data reduction was performed with the Bruker Apex3 Suite, the structures were solved with ShelXT[47] and refined with ShelXL.[48] Olex2 was used as user interface.[49] The cif files were edited with enCIFer v. 1.4,[50] and molecular graphics were produced with Diamond v. 4.6.2.

Deposition Numbers 2003219 (for **4e-Cd-DBU**), 2003220 (for **3d-Zn-*N*-MeIm**), 2003221 (for **4a-Zn**), 2003222 (for **3e-Zn-TMG**), 2003223 (for **4b-Cd-DMSO-MeOH**), 2003224 (for **4a-Cd**), 2003225 (for **3d-Zn-TBD**), 2003226 (for **4e-Zn-DBU**), 2003227 (for **3e**), 2003228 (for **3e-Zn-DMAP**), 2003229 (for **3b**) contain the supplementary crystallographic data for this paper. These data are provided free of charge by the joint Cambridge Crystallographic Data Centre and Fachinformationszentrum Karlsruhe Access Structures service www.ccdc.cam.ac.uk/structures.

The data are summarized in Table S1–S11, SI.

Experimental and analytical data for a selection of the compounds described within the text are presented here, data for all compounds can be found in the SI.

General procedure for the synthesis of Schiff base ligands 3a–3o and 4a–4g: Amine **2a** or **2b** (1.0–15 mmol) and salicylaldehyde derivative (2.0–2.2 equiv.) were mixed in EtOH (10 mL pr. mmol amine). Formic acid (5–30 drops) was added, and the suspension was stirred at reflux temperature for 20 hours. After cooling to r.t., the solids were filtered off, washed with EtOH, air dried and recrystallized to yield the Schiff base ligand. **Example (4a)**: Amine **2a** (0.671 g, 2.04 mmol, 1.0 equiv.) and 5-bromosalicylaldehyde (0.867 g, 4.31 mmol, 2.1 equiv.) were used. **4a** was obtained as orange crystals after recrystallization from MeCN (1.24 g, 1.79 mmol, 87 %). M.p. 205–206 °C; ^{1}H NMR (400 MHz, $CDCl_3$): δ = 12.13 (s, 2H, O**H**), 8.40 (s, 2H, **H^{d}**), 8.08 (dd, $^{3}J_{H,H}$ = 7.9 Hz, $^{4}J_{H,H}$ = 1.5 Hz, 2H, **H^{b}**), 7.89 (d, $^{4}J_{H,H}$ = 1.5 Hz, 2H, **H^{a}**), 7.48 (d, $^{3}J_{H,H}$ = 7.9 Hz, 2H, **H^{c}**), 7.39 (dd, $^{3}J_{H,H}$ = 8.8 Hz, $^{4}J_{H,H}$ = 2.4 Hz, 2H, **H^{f}**), 7.12 (d, $^{4}J_{H,H}$ = 2.4 Hz, 2H, **H^{h}**), 6.74 (d, $^{3}J_{H,H}$ = 8.8 Hz, 2H, **H^{e}**), 4.45 (q, $^{3}J_{H,H}$ = 7.1 Hz, 4H, $CO_2CH_2CH_3$), 1.45 ppm (t, $^{3}J_{H,H}$ = 7.1 Hz, 6H, $CO_2CH_2CH_3$); ^{13}C NMR (101 MHz, $CDCl_3$): δ = 165.7 (**C**$O_2CH_2CH_3$), 162.8 (**C^{7}**), 159.6 (**C^{9}**), 147.0 (**C^{2}**), 138.3 (**C^{1}**), 136.0 (**C^{11}**), 134.3 (**C^{13}**), 132.1 (**C^{4}**), 131.0 (**C^{6}**), 128.2 (**C^{5}**), 120.4 (**C^{8}**), 119.3 (**C^{3}**), 118.9 (**C^{10}**), 110.9 (**C^{12}**), 61.5 ($CO_2CH_2CH_3$), 14.4 ppm ($CO_2CH_2CH_3$); IR (KBr): $\tilde{\nu}$ = 1617.9 cm^{-1}; LRMS (ESI): *m/z* (%): 693.0 (42) $[M + H]^+$; HRMS (ESI): *m/z* calcd. for $C_{32}H_{26}Br_2N_2O_6$ + H: 693.0230 $[M + H]^+$, found 693.0217.

General procedure for the synthesis of Zn complexes 3a-Zn–3m-Zn and 4a-Zn–4g-Zn, and Cd complex 4b-Cd: Schiff base ligand (0.50–10 mmol, 1.0 equiv.) was suspended in MeOH (10 mL pr. mmol ligand), NEt_3 (2.2–3.6 equiv.) and then $Zn(OAc)_2{\cdot}2H_2O$ or $CdCl_2$ (1.0–1.1 equiv.) were added. The resulting suspension was stirred at r.t. for 20–24 h. The solids were filtered off, washed with MeOH, air dried and recrystallized to yield the metal complex. **Example (4a-Zn)**: Ligand **4a** (0.733 g, 1.05 mmol, 1.0 equiv.), $Zn(OAc)_2{\cdot}2H_2O$ (0.238 g, 1.08 mmol, 1.0 equiv.) and NEt_3 (0.33 mL, 2.4 mmol, 2.2 equiv.) were used. **4a-Zn** was obtained as yellow crystals after recrystallization from MeCN (0.610 g, 0.805 mmol, 76 %). M.p. 213–214 °C; ^{1}H NMR (400 MHz, [D$_6$]DMSO): δ = 8.32 (s, 2H, **H^{d}**), 7.92 (dd, $^{3}J_{H,H}$ = 8.0 Hz, $^{4}J_{H,H}$ = 1.6 Hz, 2H, **H^{b}**), 7.61 (d, $^{4}J_{H,H}$ = 1.6 Hz, 2H, **H^{a}**), 7.44–7.46 (m, 4H, **H^{c}**, **H^{h}**), 7.28 (dd, $^{3}J_{H,H}$ = 9.1 Hz, $^{4}J_{H,H}$ = 2.8 Hz, 2H, **H^{f}**), 6.56 (d, $^{3}J_{H,H}$ = 9.1 Hz, 2H, **H^{e}**), 4.27–4.37 (m, 4H, $CO_2CH_2CH_3$), 1.31 ppm (t, $^{3}J_{H,H}$ = 7.1 Hz, 6H, $CO_2CH_2CH_3$); ^{13}C NMR (101 MHz, [D$_6$]DMSO): δ = 170.3 (**C^{7}**, **C^{9}**), 164.9 (**C**$O_2CH_2CH_3$), 148.4 (**C^{2}**), 137.5 (**C^{13}**), 137.2 (**C^{11}**), 136.3 (**C^{1}**), 131.2 (**C^{6}**), 131.0 (**C^{4}**), 127.0 (**C^{5}**), 125.0 (**C^{10}**), 124.0 (**C^{3}**), 120.2 (**C^{8}**), 102.8 (**C^{12}**), 61.1 ($CO_2CH_2CH_3$), 14.1 ppm ($CO_2CH_2CH_3$); IR (KBr): $\tilde{\nu}$ = 1610.9 cm^{-1}; LRMS (ESI): *m/z* (%): 778.9 (100) $[M + Na]^+$, 1536.8 (22) $[2M + Na]^+$; HRMS (ESI): *m/z* calcd. for $C_{32}H_{24}Br_2N_2O_6Zn$ + Na: 776.9185 $[M + Na]^+$, found 776.9191; elemental analysis calcd. (%) for $C_{32}H_{24}Br_2N_2O_6Zn$: C 50.72, H 3.19, N 3.70; found C 51.02, H 2.93, N 3.53.

General procedure for synthesis of base-ligated Zn and Cd complexes (direct method): Schiff base ligand (0.50–1.0 mmol, 1.0 equiv.) was suspended in MeOH or EtOH (10–20 mL pr. mmol ligand), base (3.0–4.8 equiv.) and then $Zn(OAc)_2{\cdot}2H_2O$ or $Cd(OAc)_2{\cdot}2H_2O$ or $CdCl_2$ (1.0–1.1 equiv.) were added. The resulting suspension was stirred at r.t. for 20–24 h. The solids were filtered off, washed with MeOH or EtOH, air dried and recrystallized to yield the base-ligated metalcomplex. **Example (3d-Zn-DBU)**: Ligand **3d** (0.309 g, 0.498 mmol, 1.0 equiv.) was suspended in MeOH (10 mL). DBU (0.30 mL, 2.0 mmol, 4.0 equiv.) and then $Zn(OAc)_2{\cdot}2H_2O$ (0.120 g, 0.547 mmol, 1.1 equiv.) were added. The resulting suspension was stirred at r.t. for 24 h. The solids were filtered off and washed with MeOH. **3d-Zn-DBU** was obtained as yellow crystals after recrystallization from MeCN (0.237 g, 0.283 mmol, 57 %). M.p. 182–183 °C; ^{1}H NMR (600 MHz, $CDCl_3$): δ = 8.12 (s, 2H, **H^{d}**), 7.92 (dd, $^{3}J_{H,H}$ = 7.9 Hz, $^{4}J_{H,H}$ = 1.1 Hz, 2H, **H^{b}**), 7.63 (s, 2H, **H^{a}**), 7.25–7.31 (m, 4H, **H^{c}**, **H^{f}**), 6.92 (d, $^{3}J_{H,H}$ = 7.5 Hz, 2H, **H^{h}**), 6.38–6.41 (m, 2H, **H^{g}**), 3.92 (s, 6H, CO_2CH_3), 2.27–3.47 (m, 6H, **H^{α}**, **H^{ι}**, **H^{γ}**), 0.43–2.12 ppm (m, 28H, C(CH_3)$_3$, **H^{β}**, **H^{ε,}** **H^{ζ}**, **H^{η}**, **H^{θ}**); ^{13}C NMR (151 MHz, $CDCl_3$): δ = 172.5 (**C^{7}**, **C^{9}**), 166.2 (**C**O_2CH_3), 163.5 (**C^{δ}**), 150.0 (**C^{2}**), 142.8 (**C^{10}**), 137.7 (**C^{1}**), 134.1 (**C^{13}**), 131.3 (**C^{4}**, **C^{6}**, **C^{11}**), 126.7 (**C^{5}**), 124.3 (**C^{3}**), 118.9 (**C^{8}**), 112.2 (**C^{12}**), 53.0 (**C^{ι}**), 52.3 (CO_2CH_3), 48.1 (**C^{α}**), 42.8 (**C^{γ}**), 35.5 (**C^{ε}**), 35.3 (**C**(CH_3)$_3$), 29.2 (C(**C**H$_3$)$_3$), 29.1 (**C^{η}** or **C^{θ}**), 27.8 (**C^{η}** or **C^{θ}**), 24.3 (**C^{ζ}**), 21.1 ppm (**C^{β}**). Most of the ^{1}H and ^{13}C NMR resonances were broadened. HRMS (ESI): *m/z* calcd. for $C_{47}H_{54}N_4O_6Zn$ + H: 835.3408 $[M + H]^+$; found 835.3409; elemental analysis calcd. (%) for $C_{47}H_{54}N_4O_6$: C 67.50, H 6.51, N 6.70; found C 67.54, H 6.49, N 6.67.

General procedure for synthesis of base-ligated Zn complexes (indirect method): Zn complex **3d-Zn** or **3e-Zn** (0.25–0.50 mmol, 1.0 equiv.) was suspended in MeCN (5–10 mL). Base (1.1–3.8 equiv.) was added and the mixture was boiled until everything was dissolved (more MeCN was added if necessary). The hot solution was cooled slowly to r.t., and then further at 4 °C. After 1–2 days, the precipitated crystals were filtered off, washed with MeCN, yielding the base-ligated Zn complex. **Example (3d-Zn-*N*-MeIm)**: **3d-Zn** (0.229 g, 0.335 mmol, 1.0 equiv.) was suspended in MeCN (10 mL). *N*-MeIm (0.103 g, 1.25 mmol, 3.7 equiv.) was added and the mixture was boiled until everything had dissolved. The solution was then cooled to r.t. slowly, and then further at 4 °C for 1 day. The precipitated crystals were then filtered off and washed with MeCN. This gave **3d-Zn-*N*-MeIm** as yellow crystals, suitable for single-crystal X-ray diffraction analysis (0.158 g, 0.206 mmol, 62 %). M.p. 184–186 °C; ^{1}H NMR (600 MHz, $CDCl_3$, 2.6×10^{-3} mM): δ = 8.24 (s, 2H, **H^{d}**), 7.98

© 2020 The Authors published by Wiley-VCH GmbH

(dd, $^3J_{H,H}$ = 8.0 Hz, $^4J_{H,H}$ = 1.6 Hz, 2H, **H^{b}**), 7.75 (d, $^4J_{H,H}$ = 1.6 Hz, 2H, **H^{a}**), 7.35–7.37 (m, 3H, **H^{f}**, **H$^{\gamma}$**), 7.33 (d, $^3J_{H,H}$ = 8.0 Hz, 2H, **H^{c}**), 7.00 (dd, $^3J_{H,H}$ = 7.9 Hz, $^4J_{H,H}$ = 1.7 Hz, 2H, **H^{h}**), 6.97 (s, 1H, **H$^{\alpha}$**), 6.84 (s, 1H, **H$^{\beta}$**), 6.52–6.54 (m, 2H, **H^{g}**), 3.94 (s, 6H, CO_2CH_3), 3.66 (s, 3H, NCH_3), 1.37 ppm (s, 18H, $C(CH_3)_3$); ^{13}C NMR (151 MHz, $CDCl_3$, 2.6×10^{-3} M): δ = 172.0 (**C^{7}**), 171.9 (**C^{9}**), 166.0 (CO_2CH_3), 148.5 (**C^{2}**), 142.8 (**C^{10}**), 137.8 (**C^{1}**), 137.7 (**C$^{\gamma}$**), 134.6 (**C^{13}**), 132.7 (**C^{11}**), 132.4 (**C^{6}**), 132.0 (**C^{4}**), 129.3 (**C$^{\alpha}$**), 127.7 (**C^{5}**), 123.6 (**C^{3}**), 120.0 (**C$^{\beta}$**), 118.4 (**C^{8}**), 114.1 (**C^{12}**), 52.5 (CO_2CH_3), 35.3 ($C(CH_3)_3$), 33.3 (NCH_3), 29.2 ppm ($C(CH_3)_3$); LRMS (ESI): *m/z* (%): 705.191 [**3d-Zn** + Na]$^+$ (100), 765.263 (43) [M + H]$^+$; HRMS (ESI): *m/z* calcd. for $C_{42}H_{44}N_4O_6Zn$ + H: 765.2625 [M + H]$^+$; found 765.2626; elemental analysis calcd. (%) for $C_{45}H_{48}N_4O_6Zn$: C 65.84, H 5.79, N 7.31; found C 65.59, H 5.76, N 7.27.

Acknowledgments

The Research Council of Norway is kindly acknowledged for funding through project no. 228157 (stipend to K. T. H). This work was also partly supported by the Research Council of Norway through the Norwegian NMR Package in 1994 and partly supported by the Research Council of Norway through the Norwegian NMR Platform, NNP (226244/F50). Additional support by the Department of Chemistry and the Faculty of Mathematics and Natural Sciences at University of Oslo is also acknowledged. We thank Senior Engineer Dirk Petersen, University of Oslo, for assistance with the variable temperature NMR experiments. Furthermore, we thank Principal Engineer Osamu Sekiguchi, University of Oslo, for performing the MS experiments, and Prof. Frode Rise, University of Oslo, for providing generous access to the NMR facilities. We acknowledge use of the Norwegian National Centre for X-ray Diffraction and Scattering (RECX).

Keywords: Zinc · Schiff base ligands · 2,2′-Diaminobiphenyls · Nitrogen bases · Cadmium

[1] a) D. J. Darensbourg, P. Rainey, J. Yarbrough, *Inorg. Chem.* **2001**, *40*, 986–993; b) Y. Xu, M. Xiao, S. Wang, M. Pan, Y. Meng, *Polym. Chem.* **2014**, *5*, 3838–3846; c) A. Decortes, M. Martínez Belmonte, J. Benet-Buchholz, A. W. Kleij, *Chem. Commun.* **2010**, *46*, 4580–4582; d) M. Taherimehr, A. Decortes, S. M. Al-Amsyar, W. Lueangchaichaweng, C. J. Whiteoak, E. C. Escudero-Adán, A. W. Kleij, P. P. Pescarmona, *Catal. Sci. Technol.* **2012**, *2*, 2231–2237; e) D. Anselmo, E. C. Escudero-Adán, M. Martínez Belmonte, A. W. Kleij, *Eur. J. Inorg. Chem.* **2012**, 4694–4700; f) Y.-M. Shen, W.-L. Duan, M. Shi, *J. Org. Chem.* **2003**, *68*, 1559–1562; g) L.-Q. Lu, X.-F. Wu, in *Zinc Catalysis* (Eds.: S. Enthaler, X.-F. Wu), Wiley-VCH, Weinheim, **2015**, pp. 57–82; h) P. G. Cozzi, *Angew. Chem. Int. Ed.* **2003**, *42*, 2895–2898; *Angew. Chem.* **2003**, *115*, 3001–3004; i) F. H. Zelder, J. Rebek Jr., *Chem. Commun.* **2006**, 753–754.

[2] a) E. Martin, M. Martínez Belmonte, E. C. Escudero-Adán, A. W. Kleij, *Eur. J. Inorg. Chem.* **2014**, 4632–4641; b) A. W. Kleij, M. Kuil, D. M. Tooke, M. Lutz, A. L. Spek, J. N. H. Reek, *Chem. Eur. J.* **2005**, *11*, 4743–4750; c) A. W. Kleij, M. Kuil, M. Lutz, D. M. Tooke, A. L. Spek, P. C. J. Kamer, P. W. N. M. van Leeuwen, J. N. H. Reek, *Inorg. Chim. Acta* **2006**, *359*, 1807–1814; d) A. W. Kleij, M. Kuil, D. M. Tooke, A. L. Spek, J. N. H. Reek, *Inorg. Chem.* **2007**, *46*, 5829–5831; e) A. W. Kleij, *Dalton Trans.* **2009**, 4635–4639; f) L. Leoni, A. Dalla Cort, *Inorganics* **2018**, *6*, 42.

[3] a) E. C. Escudero-Adán, J. Benet-Buchholz, A. W. Kleij, *Inorg. Chem.* **2008**, *47*, 4256–4263; b) M. E. Germain, T. R. Vargo, P. G. Khalifah, M. J. Knapp, *Inorg. Chem.* **2007**, *46*, 4422–4429; c) J. A. Connor, M. Charlton, D. C. Cupertino, A. Lienke, M. McPartlin, I. J. Scowen, P. A. Tasker, *J. Chem. Soc., Dalton Trans.* **1996**, 2835–2838; d) A. Dalla Cort, L. Mandolini, C. Pasquini, K. Rissanen, L. Russo, L. Schiaffino, *New J. Chem.* **2007**, *31*, 1633–1638; e) H.-C. Lin, C.-C. Huang, C.-H. Shi, Y.-H. Liao, C.-C. Chen, Y.-C. Lin, Y.-H. Liu, *Dalton Trans.* **2007**, 781–791.

[4] a) G. Forte, I. P. Oliveri, G. Consiglio, S. Failla, S. Di Bella, *Dalton Trans.* **2017**, *46*, 4571–4581; b) I. P. Oliveri, G. Maccarrone, S. Di Bella, *J. Org. Chem.* **2011**, *76*, 8879–8884; c) I. P. Oliveri, S. Di Bella, *Dalton Trans.* **2017**, *46*, 11608–11614; d) G. Consiglio, S. Failla, P. Finocchiaro, I. P. Oliveri, S. D. Bella, *Dalton Trans.* **2012**, *41*, 387–395; e) E. C. Escudero-Adán, J. Benet-Buchholz, A. W. Kleij, *Chem. Eur. J.* **2009**, *15*, 4233–4237.

[5] a) P. G. Cozzi, *Chem. Soc. Rev.* **2004**, *33*, 410–421; b) G. Consiglio, I. P. Oliveri, S. Failla, S. Di Bella, *Molecules* **2019**, *24*, 2514.

[6] a) S. G. Telfer, R. Kuroda, *Coord. Chem. Rev.* **2003**, *242*, 33–46; b) C.-M. Che, J.-S. Huang, *Coord. Chem. Rev.* **2003**, *242*, 97–113; c) P. D. Knight, P. Scott, *Coord. Chem. Rev.* **2003**, *242*, 125–143.

[7] a) S. L. James, *Chem. Soc. Rev.* **2003**, *32*, 276–288; b) H.-C. Zhou, J. R. Long, O. M. Yaghi, *Chem. Rev.* **2012**, *112*, 673–674; c) N. Stock, S. Biswas, *Chem. Rev.* **2012**, *112*, 933–969.

[8] a) J. Hassan, M. Sévignon, C. Gozzi, E. Schulz, M. Lemaire, *Chem. Rev.* **2002**, *102*, 1359–1470; b) R. R. González, L. Liguori, A. M. Carrillo, H.-R. Bjørsvik, *J. Org. Chem.* **2005**, *70*, 9591–9594; c) M. E. Bouillon, H. H. Meyer, *Tetrahedron* **2016**, *72*, 3151–3161; d) V. Elumalai, H.-R. Bjørsvik, *ChemistrySelect* **2017**, *2*, 9387–9390; e) L. Schulz, M. Enders, B. Elsler, D. Schollmeyer, K. M. Dyballa, R. Franke, S. R. Waldvogel, *Angew. Chem. Int. Ed.* **2017**, *56*, 4877–4881; *Angew. Chem.* **2017**, *129*, 4955–4959; f) T. Chatterjee, G.-b. Roh, M. A. Shoaib, C.-H. Suhl, J. S. Kim, C.-G. Cho, E. J. Cho, *Org. Lett.* **2017**, *19*, 1906–1909; g) Y. Shi, J. Liu, Y. Yang, J. You, *Chem. Commun.* **2019**, *55*, 5475–5478; h) K. T. Hylland, S. Øien-Ødegaard, M. Tilset, *Eur. J. Org. Chem.* **2020**, 4208–4226.

[9] C. Reichardt, *Solvents and Solvent Effects in Organic Chemistry*, 3rd ed., Wiley-VCH Verlag GmbH & Co, Weinheim, **2003**.

[10] G. Consiglio, S. Failla, P. Finocchiaro, I. P. Oliveri, S. Di Bella, *Inorg. Chem.* **2012**, *51*, 8409–8418.

[11] E. C. Escudero-Adán, J. Benet-Buchholz, A. W. Kleij, *Dalton Trans.* **2008**, 734–737.

[12] a) D. J. Darensbourg, *Chem. Rev.* **2007**, *107*, 2388–2410; b) A. Decortes, A. M. Castilla, A. W. Kleij, *Angew. Chem. Int. Ed.* **2010**, *49*, 9822–9837; *Angew. Chem.* **2010**, *122*, 10016–10032; c) J. Rintjema, L. Peña Carrodeguas, V. Laserna, S. Sopeña, A. W. Kleij, in *Carbon Dioxide and Organometallics* (Ed.: X.-B. Lu), Springer International Publishing, Cham, **2016**, pp. 39–71.

[13] S. Klaus, M. W. Lehenmeier, C. E. Anderson, B. Rieger, *Coord. Chem. Rev.* **2011**, *255*, 1460–1479.

[14] a) N. E. Searle, R. Adams, *J. Am. Chem. Soc.* **1933**, *55*, 1649–1654; b) N. Ko, J. Hong, S. Sung, K. E. Cordova, H. J. Park, J. K. Yang, J. Kim, *Dalton Trans.* **2015**, *44*, 2047–2051.

[15] a) Y. Degani, S. Dayagi, in *Carbon–Nitrogen Double Bonds (1970)* (Ed.: S. Patai), John Wiley & Sons Ltd., Great Britain, **1970**, pp. 61–147; b) R. Hernández-Molina, A. Mederos, in *Comprehensive Coordination Chemistry II* (Eds.: J. A. McCleverty, T. J. Meyer), Pergamon, Oxford, **2003**, pp. 411–446.

[16] A. W. Kleij, D. M. Tooke, A. L. Spek, J. N. H. Reek, *Eur. J. Inorg. Chem.* **2005**, 4626–4634.

[17] G. A. Morris, H. Zhou, C. L. Stern, S. T. Nguyen, *Inorg. Chem.* **2001**, *40*, 3222–3227.

[18] E. C. Constable, G. Zhang, C. E. Housecroft, M. Neuburger, J. A. Zampese, *Inorg. Chim. Acta* **2010**, *363*, 4207–4213.

[19] a) A. Okuniewski, D. Rosiak, J. Chojnacki, B. Becker, *Polyhedron* **2015**, *90*, 47–57; b) D. Rosiak, A. Okuniewski, J. Chojnacki, *Polyhedron* **2018**, *146*, 35–41.

[20] G. Zhang, Q. Li, G. Proni, *Inorg. Chem. Commun.* **2014**, *40*, 47–50.

[21] A. Mitra, P. J. Seaton, R. Ali Assarpour, T. Williamson, *Tetrahedron* **1998**, *54*, 15489–15498.

[22] G. Consiglio, S. Failla, P. Finocchiaro, I. P. Oliveri, R. Purrello, S. Di Bella, *Inorg. Chem.* **2010**, *49*, 5134–5142.

[23] a) J. P. Jesson, E. L. Muetterties, in *Dynamic Nuclear Magnetic Resonance Spectroscopy* (Eds.: L. M. Jackman, F. A. Cotton), Academic Press, **1975**, USA, pp. 253–316; b) F. A. Cotton, *Acc. Chem. Res.* **1968**, *1*, 257–265.

[24] a) R. S. Berry, *J. Chem. Phys.* **1960**, *32*, 933–938; b) R. R. Holmes, *Acc. Chem. Res.* **1979**, *12*, 257–265; c) E. P. A. Couzijn, J. C. Slootweg, A. W.

© 2020 The Authors published by Wiley-VCH GmbH

Ehlers, K. Lammertsma, *J. Am. Chem. Soc.* **2010**, *132*, 18127–18140; d) K. Nikitin, R. O'Gara, *Chem. Eur. J.* **2019**, *25*, 4551–4589.
[25] R. H. Holm, in *Dynamic Nuclear Magnetic Resonance Spectroscopy* (Eds.: L. M. Jackman, F. A. Cotton), Academic Press, **1975**, pp. 317–376.
[26] a) B. Maji, D. S. Stephenson, H. Mayr, *ChemCatChem* **2012**, *4*, 993–999; b) D. Margetic, in *Superbases for Organic Synthesis* (Ed.: T. Ishikawa), John Wiley & Sons, Ltd, United Kingdom, **2009**, pp. 9–48; c) C. Laurence, J. F. Gal, *Lewis Basicity and Affinity Scales: Data and Measurement*, John Wiley & Sons, Ltd., United Kingdom, **2010**.
[27] R. D. Sole, A. D. Luca, G. Mele, G. Vasapollo, *J. Porphyr. Phthalocyanines* **2005**, *9*, 519–527.
[28] D. Anselmo, E. C. Escudero-Adán, J. Benet-Buchholz, A. W. Kleij, *Dalton Trans.* **2010**, *39*, 8733–8740.
[29] C. Sabot, K. A. Kumar, C. Antheaume, C. Mioskowski, *J. Org. Chem.* **2007**, *72*, 5001–5004.
[30] a) S. H. Oakley, D. B. Soria, M. P. Coles, P. B. Hitchcock, *Polyhedron* **2006**, *25*, 1247–1255; b) M. P. Coles, *Dalton Trans.* **2006**, 985–1001.
[31] a) J. E. Taylor, S. D. Bull, J. M. J. Williams, *Chem. Soc. Rev.* **2012**, *41*, 2109–2121; b) T. Ishikawa, T. Kumamoto, in *Superbases for Organic Synthesis* (Ed.: T. Ishikawa), John Wiley & Sons, Ltd, United Kingdom, **2009**, pp. 49–91.
[32] J. Otera, J. Nishikido, *Esterification: Methods, Reactions and Applications*, Wiley-VCH GmbH & Co, Germany, **2010**.
[33] H. W. Horn, G. O. Jones, D. S. Wei, K. Fukushima, J. M. Lecuyer, D. J. Coady, J. L. Hedrick, J. E. Rice, *J. Phys. Chem. A* **2012**, *116*, 12389–12398.
[34] A. W. Addison, T. N. Rao, J. Reedijk, J. van Rijn, G. C. Verschoor, *J. Chem. Soc., Dalton Trans.* **1984**, 1349–1356.
[35] T. Steiner, *Angew. Chem. Int. Ed.* **2002**, *41*, 48–76; *Angew. Chem.* **2002**, *114*, 50–80.
[36] M. P. Coles, *Chem. Commun.* **2009**, 3659–3676.
[37] a) D. Dakternieks, *Coord. Chem. Rev.* **1985**, *62*, 1–35; b) J. Malito, *Annu. Rep. Prog. Chem.* **2001**, *97*, 117–131; c) I. J. Shannon, *Annu. Rep. Prog. Chem.* **2004**, *100*, 141–150; d) M. P. Coles, *Annu. Rep. Prog. Chem.* **2011**, *107*, 246–252.
[38] W. Maret, J.-M. Moulis, in *Cadmium: From Toxicity to Essentiality* (Eds.: A. Sigel, H. Sigel, R. K. O. Sigel), Springer Netherlands, Dordrecht, **2013**, pp. 1–29.
[39] H. Vahrenkamp, *Dalton Trans.* **2007**, 4751–4759.
[40] a) W.-K. Dong, Y.-X. Sun, Y.-P. Zhang, L. Li, X.-N. He, X.-L. Tang, *Inorg. Chim. Acta* **2009**, *362*, 117–124; b) S. Basak, S. Sen, C. Marschner, J. Baumgartner, S. R. Batten, D. R. Turner, S. Mitra, *Polyhedron* **2008**, *27*, 1193–1200.
[41] S. Banerjee, A. Ghosh, B. Wu, P.-G. Lassahn, C. Janiak, *Polyhedron* **2005**, *24*, 593–599.
[42] a) L. J. Alcock, G. Cavigliasso, A. C. Willis, R. Stranger, S. F. Ralph, *Dalton Trans.* **2016**, *45*, 9036–9040; b) Q. Shi, L. Xu, J. Ji, Y. Li, R. Wang, Z. Zhou, R. Cao, M. Hong, A. S. C. Chan, *Inorg. Chem. Commun.* **2004**, *7*, 1254–1257; c) P. D. Frischmann, G. A. Facey, P. Y. Ghi, A. J. Gallant, D. L. Bryce, F. Lelj, M. J. MacLachlan, *J. Am. Chem. Soc.* **2010**, *132*, 3893–3908.
[43] For examples of metal-DMSO complexes where coordination takes place via sulfur, see a) A. Abbasi, M. Y. Skripkin, L. Eriksson, N. Torapava, *Dalton Trans.* **2011**, *40*, 1111–1118; b) E. Alessio, *Chem. Rev.* **2004**, *104*, 4203–4242.
[44] a) M. Sandstrom, *Acta Chem. Scand.* **1978**, *A32*, 519–525; b) K. Moghanlou, *Acta Crystallogr., Sect. E Struct. Rep. Online* **2013**, *69*, m49; c) E. Szostak, A. Migdał-Mikuli, P. Bernard, *J. Mol. Struct.* **2015**, *1092*, 81–88.
[45] T. O. Shmakova, D. A. Garnovskii, K. A. Lysenko, E. P. Ivakhnenko, V. I. Simakov, I. S. Vasil'chenko, A. I. Uraev, A. S. Burlov, M. Y. Antipin, A. D. Garnovskii, I. E. Uflyand, *Russ. J. Coord. Chem.* **2009**, *35*, 657–662.
[46] P. D. Frischmann, M. J. MacLachlan, *Chem. Commun.* **2007**, 4480–4482.
[47] G. M. Sheldrick, *Acta Crystallogr., Sect. A* **2015**, *71*, 3–8.
[48] G. M. Sheldrick, *Acta Crystallogr., Sect. C* **2015**, *71*, 3–8.
[49] O. V. Dolomanov, L. J. Bourhis, R. J. Gildea, J. A. K. Howard, H. Puschmann, *J. Appl. Crystallogr.* **2009**, *42*, 339–341.
[50] F. H. Allen, O. Johnson, G. P. Shields, B. R. Smith, M. Towler, *J. Appl. Crystallogr.* **2004**, *37*, 335–338.

Received: June 20, 2020

© 2020 The Authors published by Wiley-VCH GmbH